

Magnetic reconnection, relaxation and particle acceleration in unstable twisted coronal loops



Philippa Browning

Jodrell Bank Centre for Astrophysics, University of Manchester

Mykola Gordovskyy, Francesca Lucini, Adam Stanier - Manchester;

Michael Bareford, Alan Hood - St Andrews;

Eduard Kontar, Nicholas Bian - Glasgow;

Ken McClements - Culham Science Centre;

Rui Pinto, Nicole Vilmer - Meudon;

Slava Lukin – NRL, NSF

- **The solar corona, flares and coronal heating**
 - Twisted fields in the corona
- **Reconnection and particle acceleration in unstable cylindrical twisted loops**
 - MHD and test particles in a single cylindrical loop
- **Realistic loop models and observational signatures**
 - Curved loops, thermodynamics and forward modelling
- **Beyond the single loop model**
 - Repeated heating events and multiple loops
 - Towards complex topologies (3D null points)

The solar corona



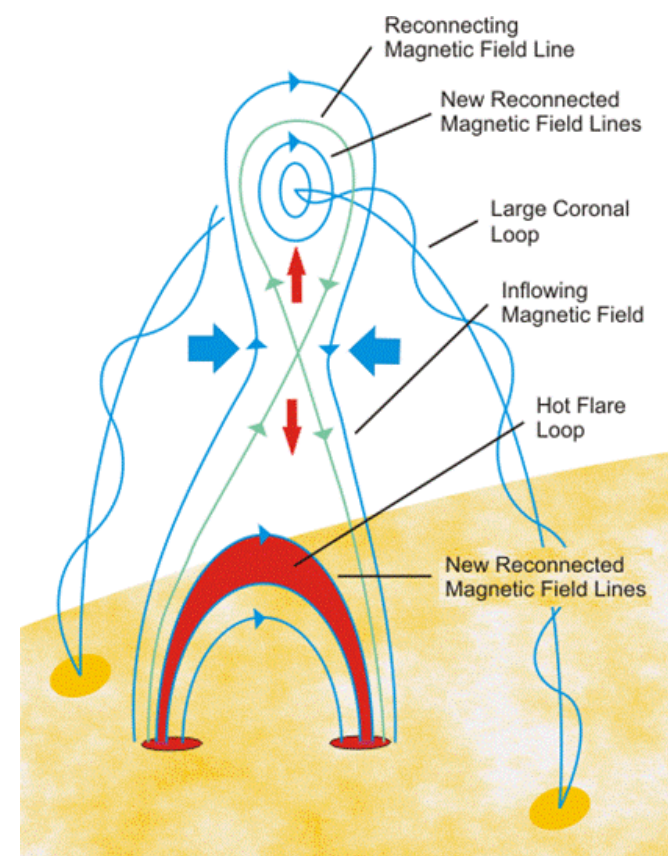
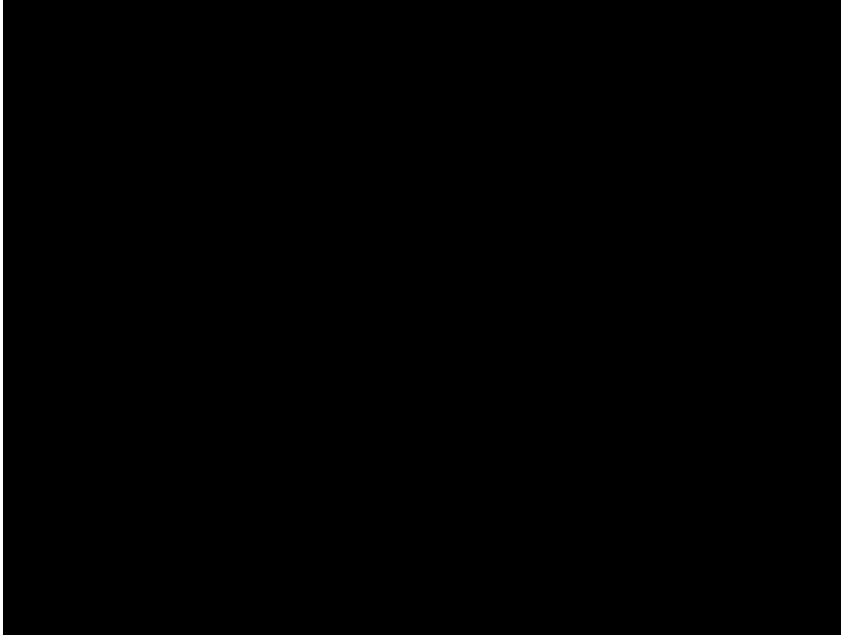
- The corona is the **hot** ($T \approx 10^6 - 10^7$ K) **tenuous** outer atmosphere of the Sun
- c.f. photosphere, $T \approx 6000$ K

• Highly dynamic and structured plasma dominated by magnetic field $\beta \ll 1$



Solar flares – magnetic reconnection in action

X class flare
September
2014



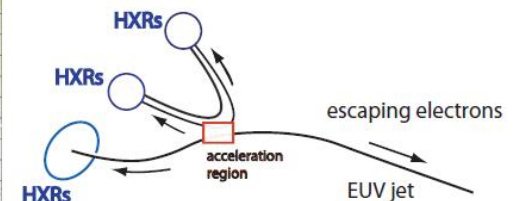
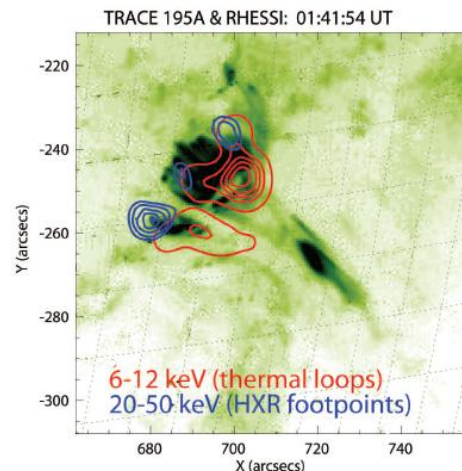
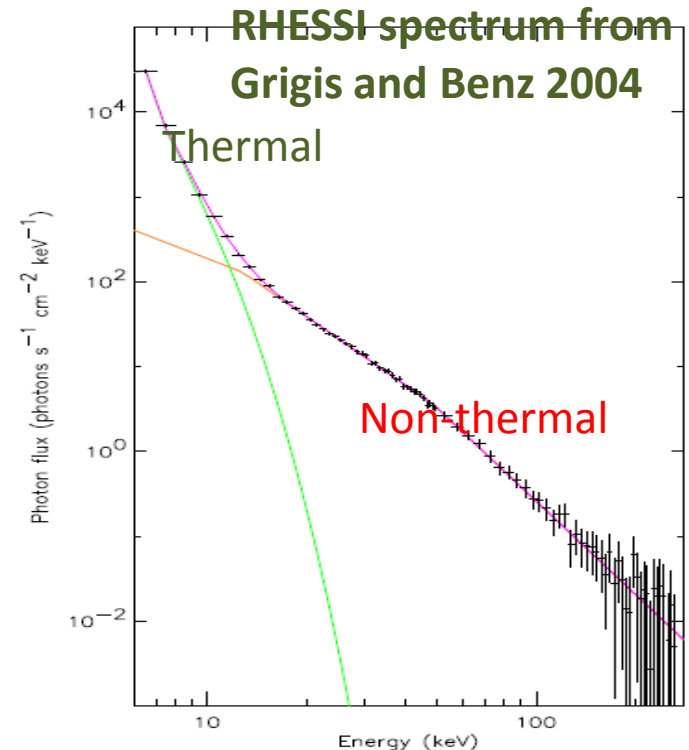
- Solar flares are dramatic events releasing up to 10^{25} J of stored magnetic energy over minutes/hours – strong brightening in soft x-rays
- Plasma heating and non-thermal energetic particles - signatures across the em spectrum from gamma rays to radio
- **Primary energy release process believed to be magnetic reconnection**

Energetic particles in solar flares

Flares produce substantial numbers of non-thermal energetic ions and electrons

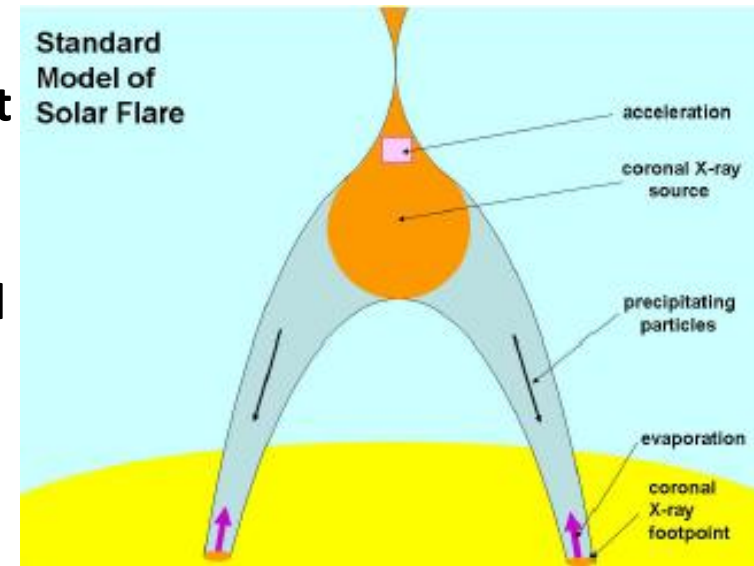
- Up to 50% of flare energy in non-thermal particles
- May propagate down to solar surface where they impact on dense chromosphere emitting bremsstrahlung - “Collisional Thick Target Model” CTTM
 - Hard X-ray emission e.g. RHESSI
- Or along open field lines into space, may be source of Solar Energetic Particles and contribute to “space weather”
 - Radio/microwave emission

RHESSI Hard X-rays and SXR
Schematic (right) from
Vlahos et al 2009

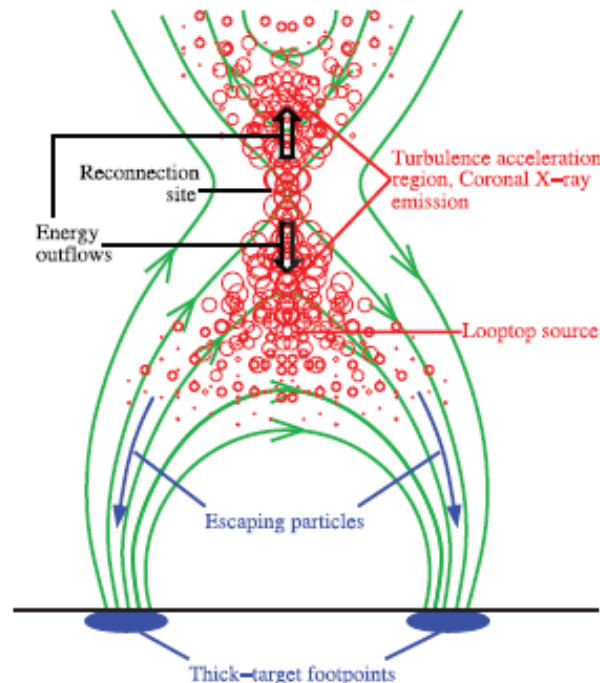


Particle acceleration mechanisms

- Strong candidate for particle acceleration is direct electric field in reconnecting current sheet (at loop top in “standard model”)
- Also proposed - waves, turbulence, shocks
- Difficulties with standard model and “Collisional Thick Target Model” - acceleration in highly-localised monolithic coronal current sheet *e.g. Brown et al 2009*
 - Number problem, intense beam....



From Liu et al 2008



• May be alleviated by chromospheric (re-) acceleration and/or distributed or stochastic acceleration *e.g. Vlahos et al 2009*

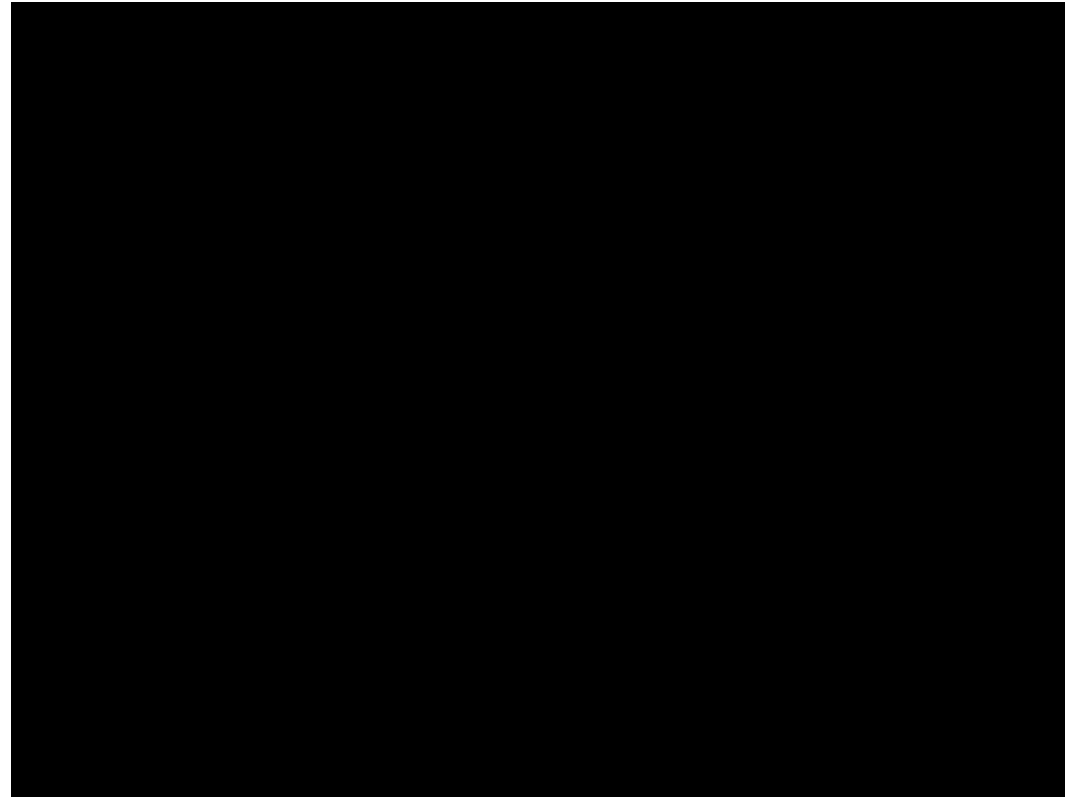
• Here bring together elements of “reconnection” and “stochastic” models - reconnection closely linked to turbulence *e.g. Browning and Lazarian, 2013*



Coronal heating and nanoflares

- Need heat source to balance losses due to conduction and radiation (T over 10^6 K)
- Sub-surface motions shuffle the footpoints of the coronal magnetic field → free magnetic energy in the corona
- For slow driving, field evolves through equilibria - free energy associated with static currents

$$\mathbf{j} \times \mathbf{B} = 0$$

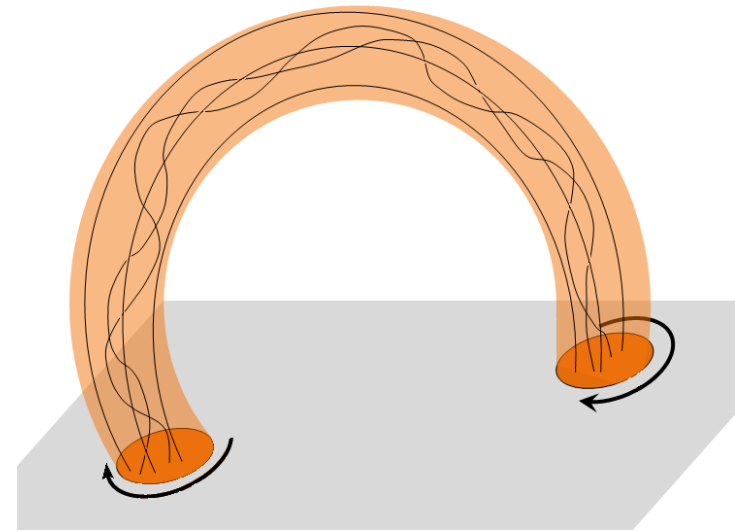
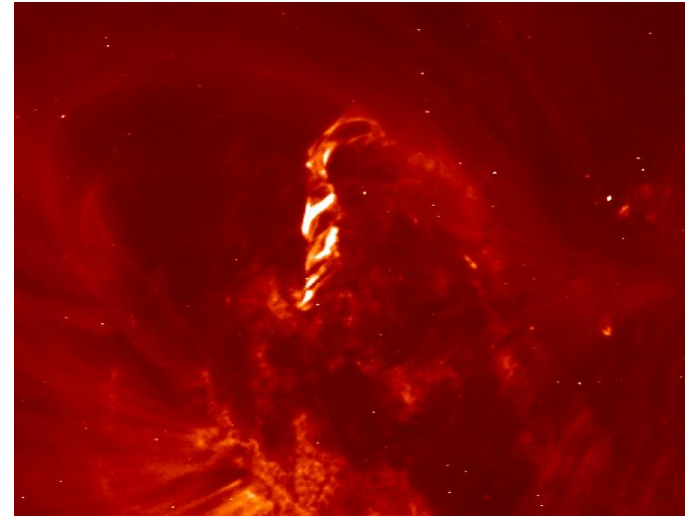


SDO Coronal loops Oct 26-29 2014

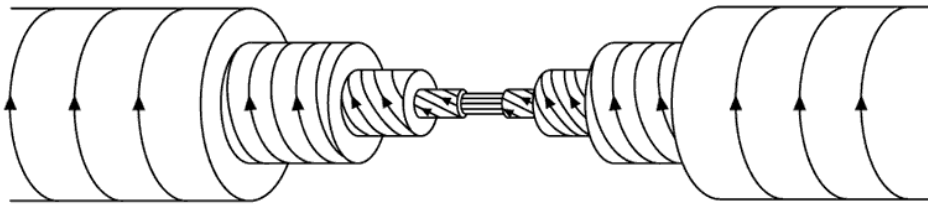
- Magnetic reconnection may dissipate this energy efficiently in highly-conducting coronal plasma
- Corona may be heated by combined effect of many small “nanoflares” (*Parker 1988*)

Twisted fields in the corona

- Non-potential coronal fields due to emergence of current-carrying flux and/or photospheric footpoint motions
- Twisted loops are observed directly in EUV *e.g. Song et al. 2008; Raouafi et al. 2009*
- Reconstructed coronal field often shows substantial twist
e.g. Regnier & Amari 2004; Malanushenko et al 2011
- Free magnetic energy associated with currents



Twisted flux ropes



Interior Structure of Flux Rope

Ubiquitous structure in laboratory, space and astrophysical plasmas

• *Russell et al (eds) Physics of magnetic flux ropes, AGU 1990*

• *Plasma Physics and Controlled Fusion Special Issue June 2014*

- Coronal Mass ejections and erupting filaments
- Solar coronal loops and flares
- Solar and stellar interiors – dynamos
- Planetary magnetospheres and solar wind
- Basic plasma physics lab experiments
 - e.g. LaPD Gekelman et al 2014; Moser and Bellan, 2012; RSX Sears et 2014....
- Spheromaks
 - e.g. Brown, Browning et al Space Sci Rev 2013
- Tokamaks, Reverse Field Pinches etc

Reconnection and particle acceleration in unstable twisted cylindrical loops

Energy release – relaxation theory

- Relaxation to a minimum energy state conserving total magnetic helicity (K)

Taylor 1974

$$K = \int_V \mathbf{A} \cdot \mathbf{B} dV$$



$$H_m = 0$$



$$H_m = T\Phi^2$$



$$H_m = \pm 2\Phi_1\Phi_2$$

From Wiegmann

Liv Rev Sol Phys

- Relaxed state is constant- α or linear force-free field

$$\nabla \times \mathbf{B} = \alpha \mathbf{B}$$

$$\alpha = \mu_0 j_{\parallel} / B$$

- Solar coronal field releases free magnetic energy as heat during relaxation from nonlinear force-free field *Heyvaerts & Priest 1984*

- Helicity is invariant in ideal MHD
- Magnetic reconnection destroys individual flux tube helicities
- Global helicity still approximately conserved in presence of small-scale reconnection – helicity dissipation much less than energy dissipation

How does relaxation happen in the corona?

- Heyvaerts-Priest assumed continuous relaxation with (unknown) timescale
- But relaxation is likely to be an intermittent process
- How far can free energy build up before onset of relaxation ?

→ heating rate

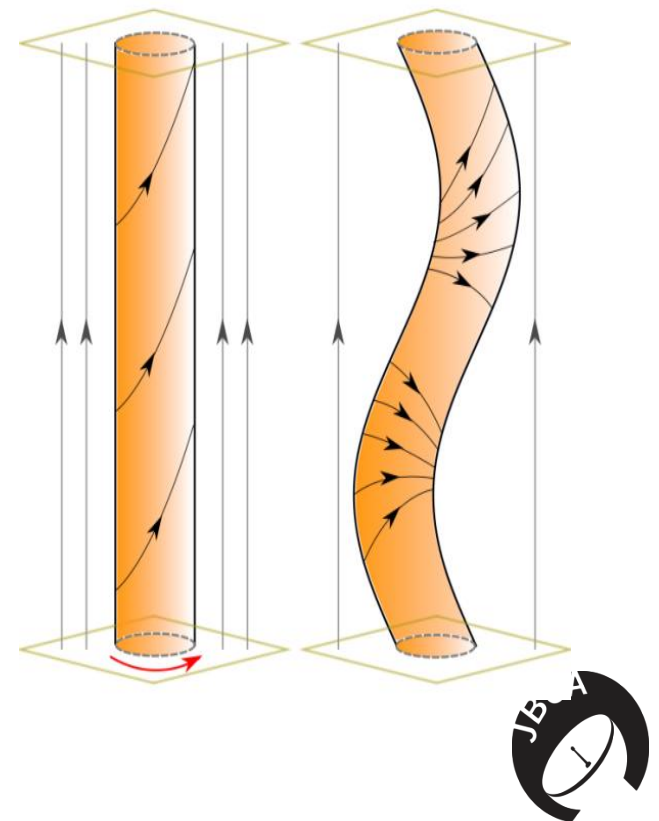
• Proposed that a possible trigger for relaxation is the onset of kink instability in a twisted coronal loop

Browning and Van der Linden 2003

• Helicity-conserving relaxation during nonlinear phase of kink instability

$$W_{heat} = W_{initial} - W_{relaxed}(\alpha)$$

where α determined by helicity conservation and $W_{initial}$ evaluated at ideal kink instability threshold



Kink-unstable twisted cylindrical coronal loop

- Solve 3D MHD equations with Lagrangian-Remap code LARE3D

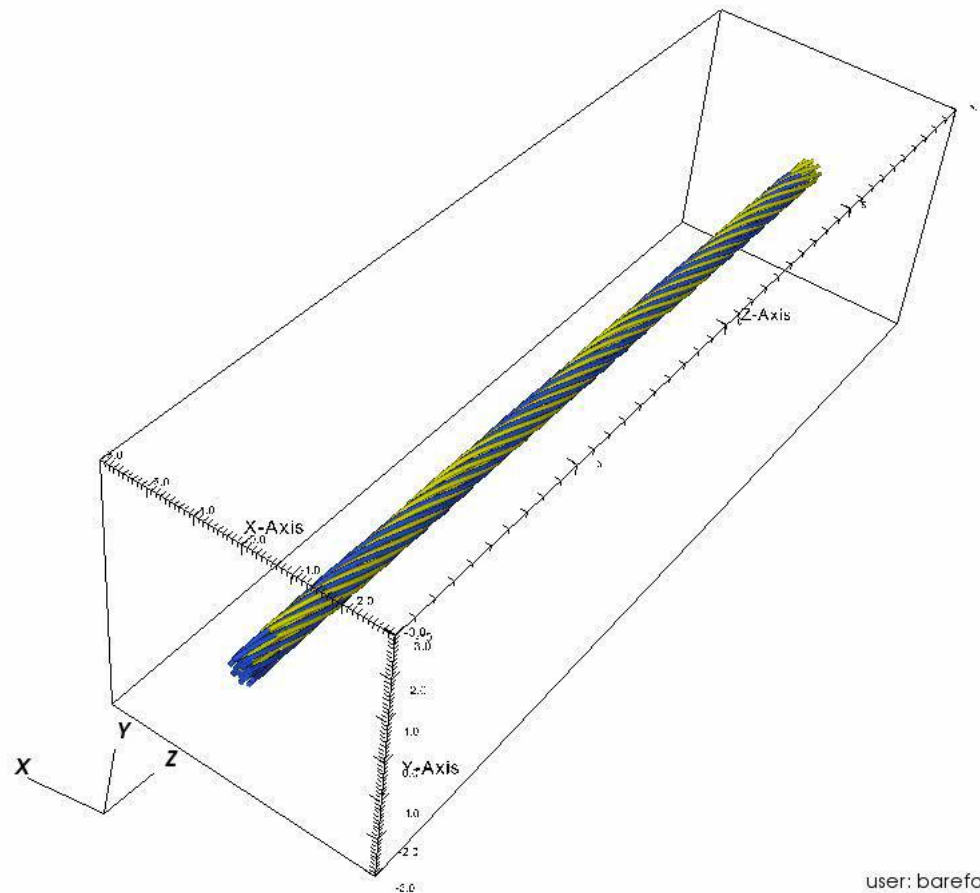
Arber et al 2001

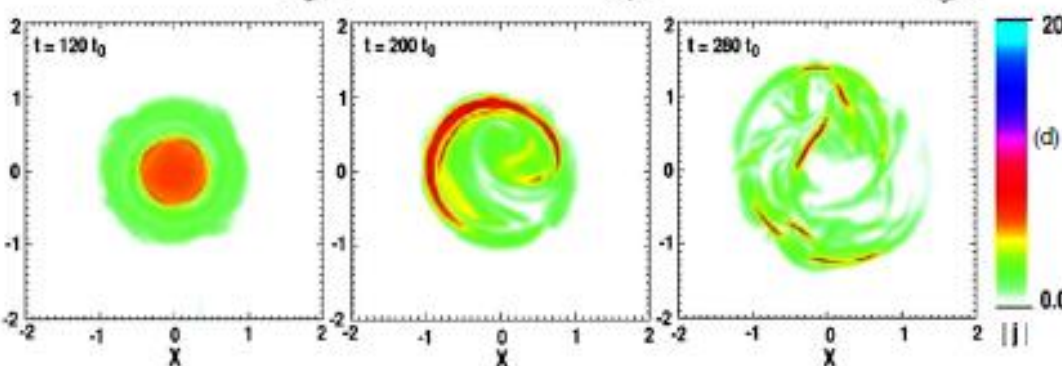
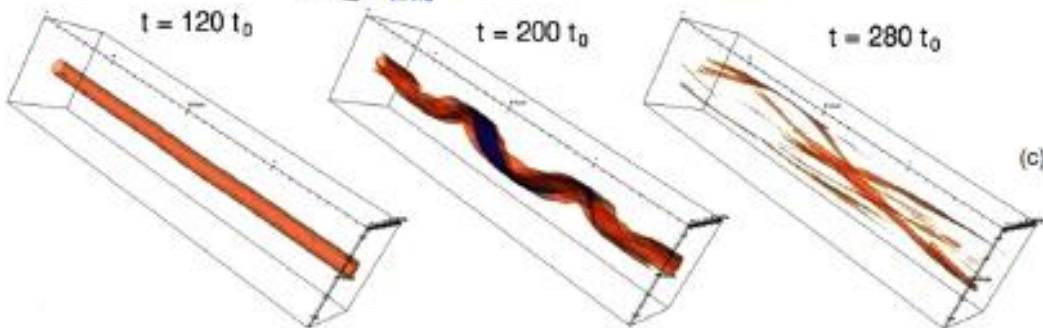
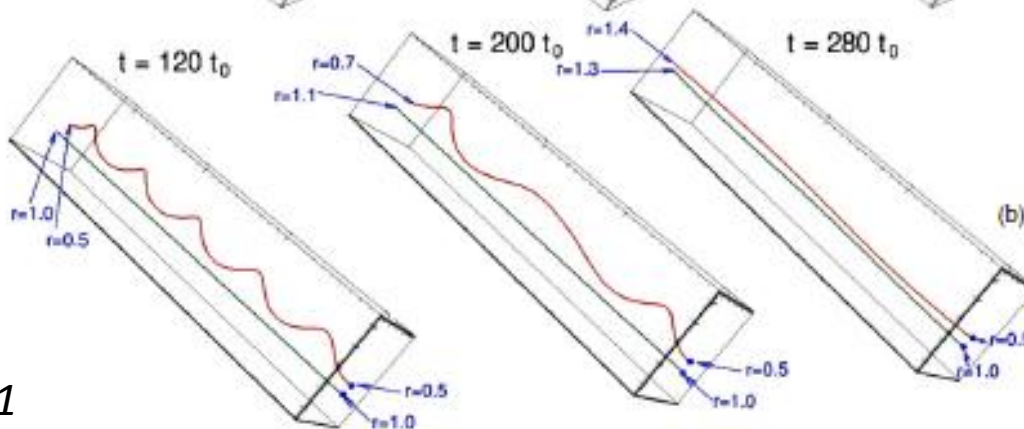
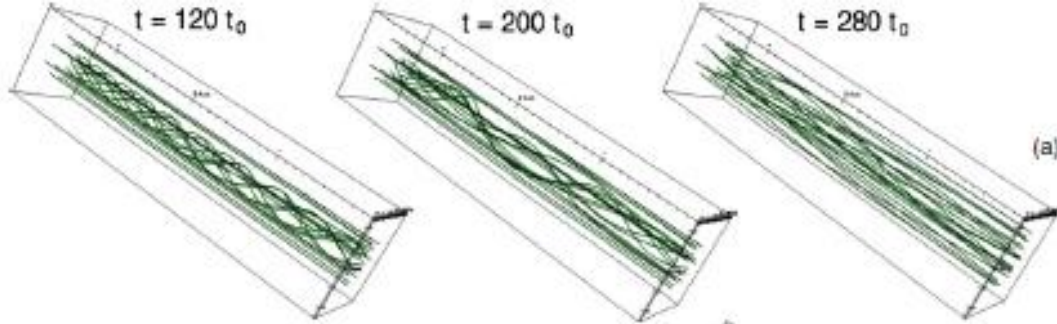
- Previous work considered initial cylindrical nonlinear force-free equilibrium with $\alpha(r)$ linearly unstable to ideal kink

Browning et al 2008, Hood et al 2009, Bareford et al 2013

- Helicity conserved much better than energy
- Final state close to “constant- α ” minimum energy state and energy release well approximated by relaxation theory

DB: 0000.IIId
Cycle: 0 Time:0





- Helical current ribbon forms at quasi-resonant surface of linear kink
- Current sheet stretches and fragments
- Reconnection within loop and with surrounding axial field \rightarrow loop expansion and “untwisting” of field
- Mixing of α -profile (relaxation to constant- α) due to multiple reconnections

Gordovskyy &
Browning 2011

Particle acceleration and transport in unstable twisted loops

- Test particles coupled to 3D MHD loop simulations
- Relativistic guiding-centre equations with time-evolving E and B - fields interpolated in (x, y, z, t)
- Particles efficiently accelerated throughout loop volume by fragmented current sheet → distributed acceleration region, avoiding some problems of “standard flare model”

Gordovsky and Browning 2011, 2012

• Recent work incorporates Coulomb collisions of test particles with background plasma – mainly in dense chromosphere

• Energy loss

Removes high energy electrons, softens spectrum

• Pitch-angle scattering

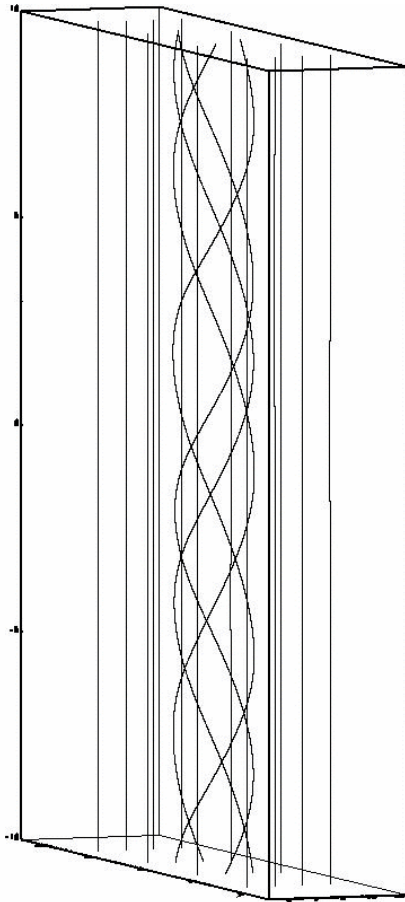
Improves confinement of energetic particles since allows mirroring at footpoints

Gordovsky et al 2013

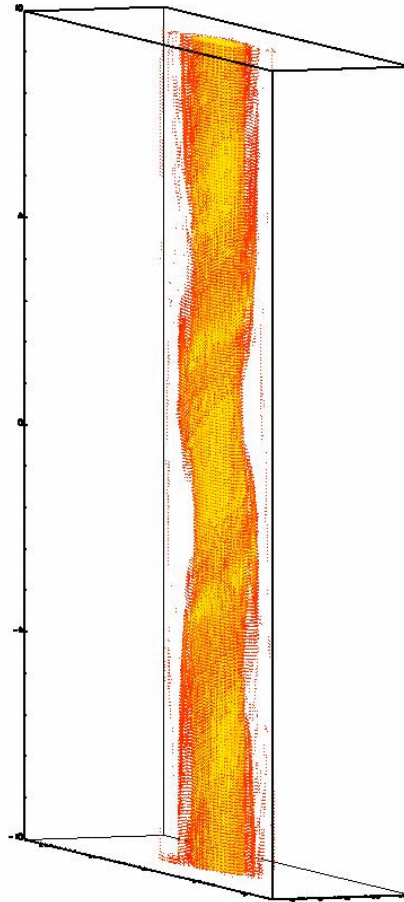
Particle distribution in space – cylindrical loop

Particles accelerated throughout loop volume by repeated encounters with fragmented current sheet *Gordovsky and Browning 2011, 2012*

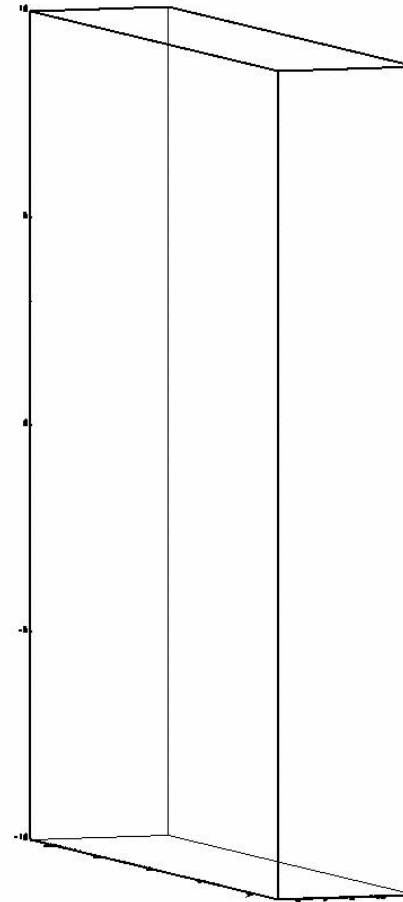
Magnetic field



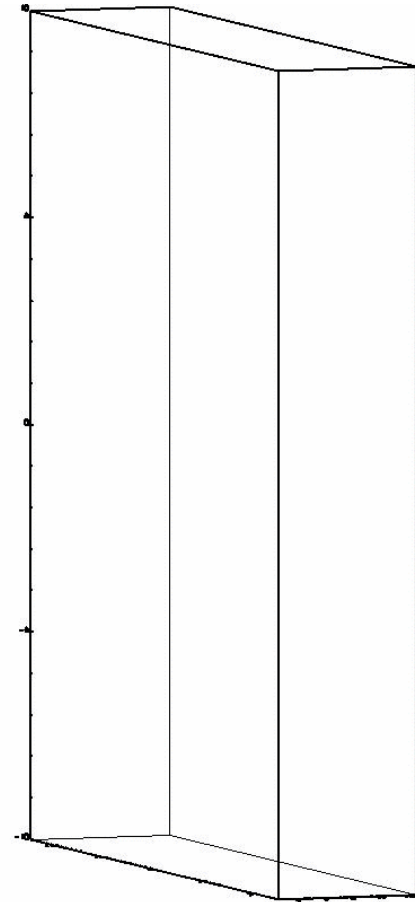
Current density



Protons



Electrons

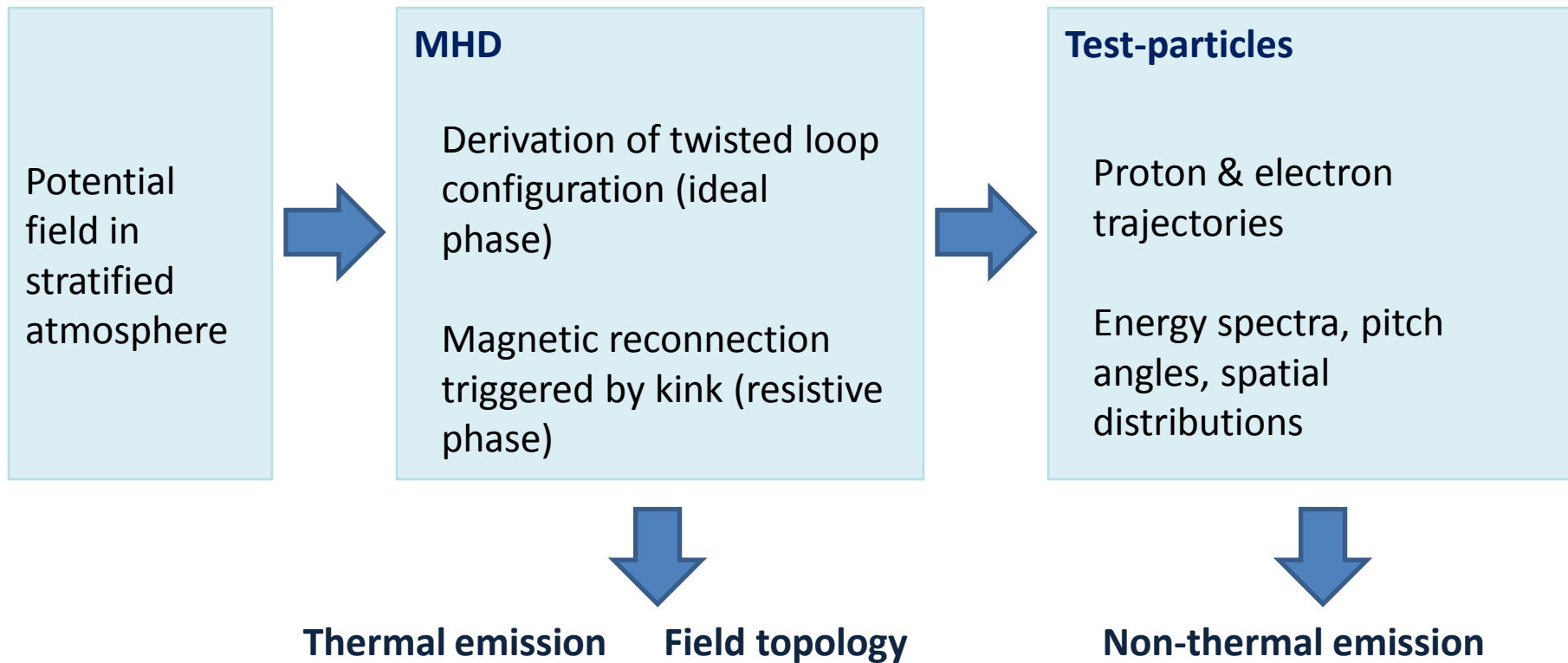


$E = 100\text{keV} \dots 1\text{MeV}$

$E > 1\text{MeV}$

Realistic loop models and observational signatures

Towards realistic models – methodology

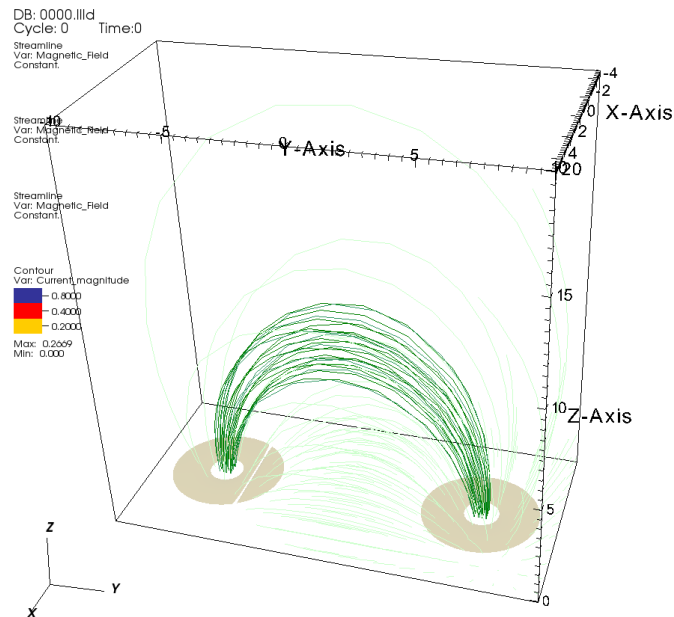


- Solve 3D MHD equations using LARE3D (Arber et al, 2001) with thermal conduction - anomalous resistivity above critical current
- Test particle calculations using relativistic guiding-centre equations including collisions with background plasma

Gordovsky, Browning, Kontar and Bian Sol Phys 2014
Gordovsky, Pinto, Browning and Vilmer in preparation

Evolution to unstable twisted loop

• Initial potential field corresponding to a “magnetic dipole” located under the photosphere



- Use ideal MHD and apply “localised” rotation at the photosphere $v_{\text{rot}} \ll v_A$
- Wait for it to kink

▪ “Switch on” resistivity before instability onset

• Anomalous resistivity above critical current due to ion acoustic instability

$$j_{\text{crit}} \propto \rho \sqrt{T}$$

• Gravitationally-stratified atmosphere

• Energy equation with conduction and optically-thin radiation

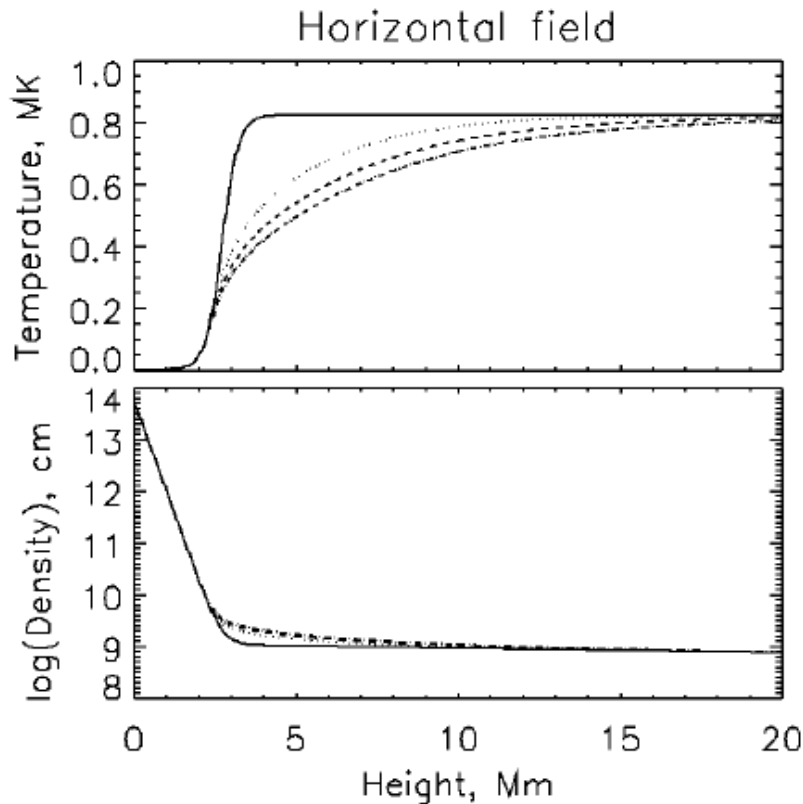
Gordovskyy, Browning, Bian and Kontar A&A 2014

Bareford, Gordovskyy, Browning and Hood 2014 in preparation

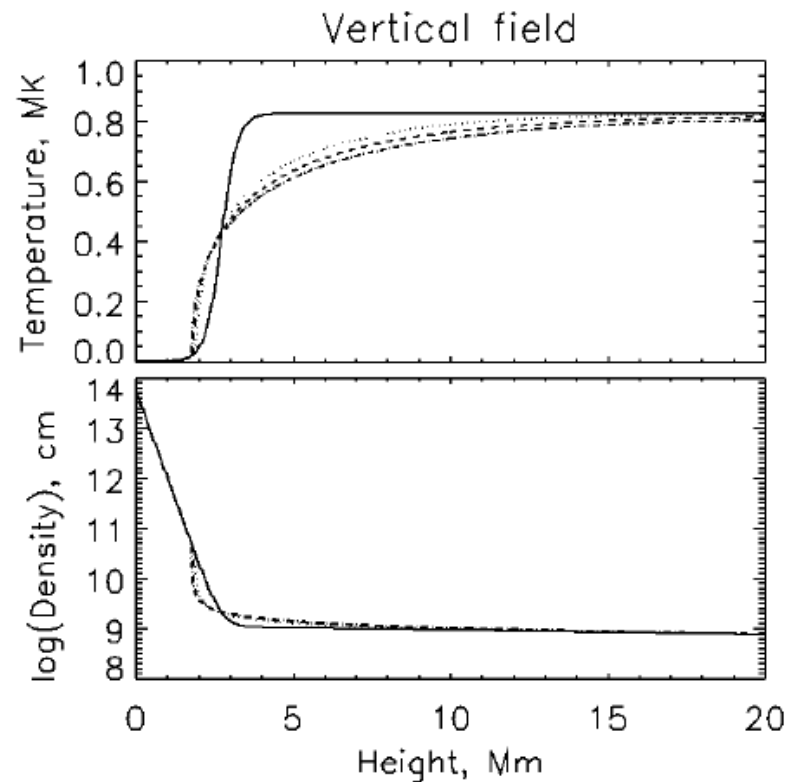
Pinto, Gordovskyy, Browning and Vilmer 2014 in preparation

Initial atmosphere

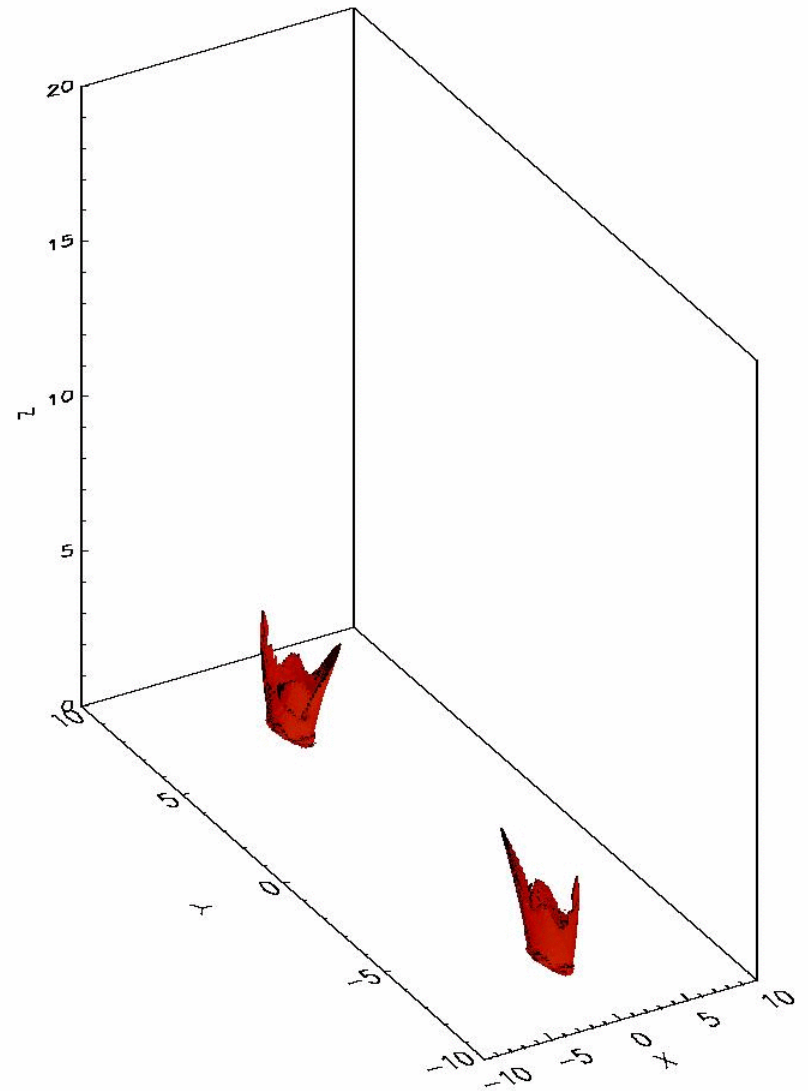
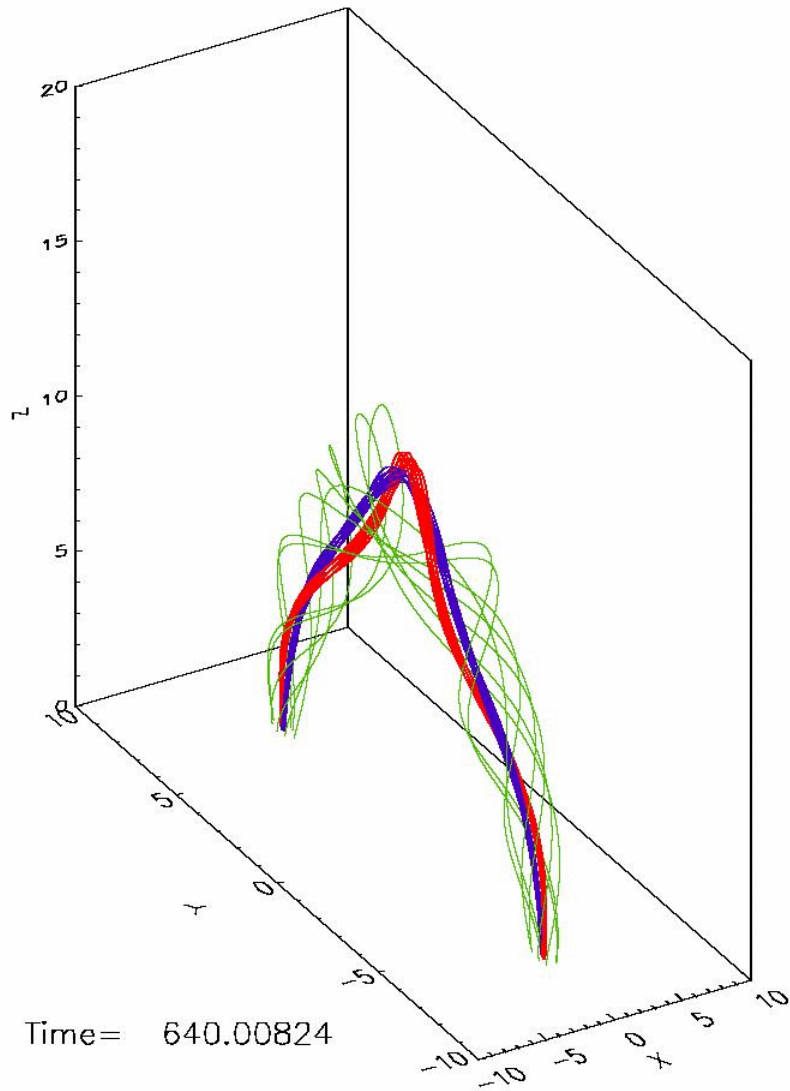
- Chromosphere to corona
- Evolve temperature and density to quasi-equilibrium before twisting loop
- Temperature profile affected by non-isotropic thermal conduction



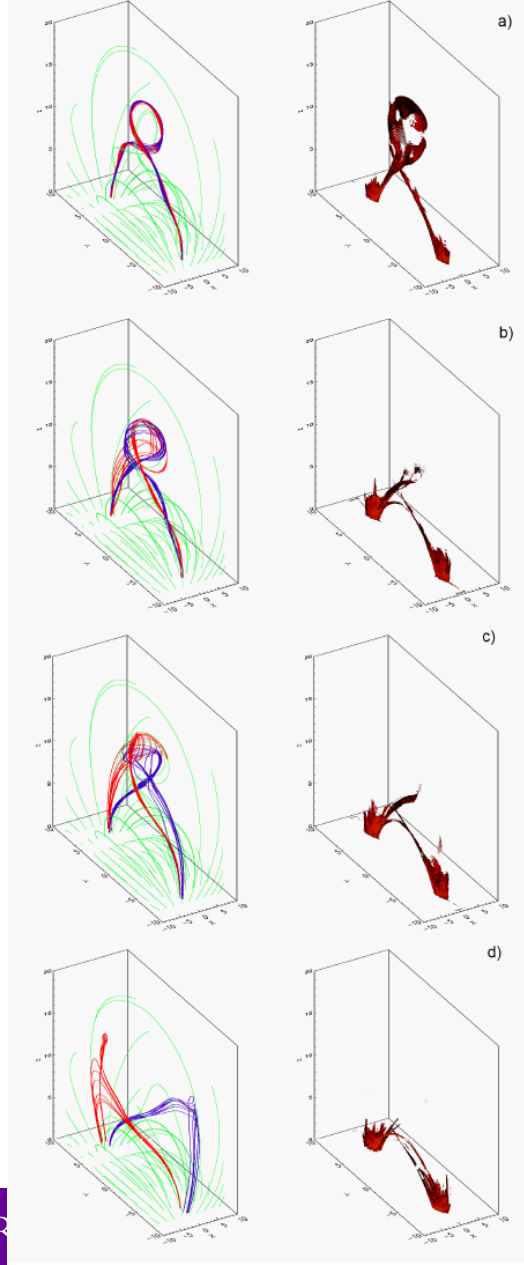
Loop midplane



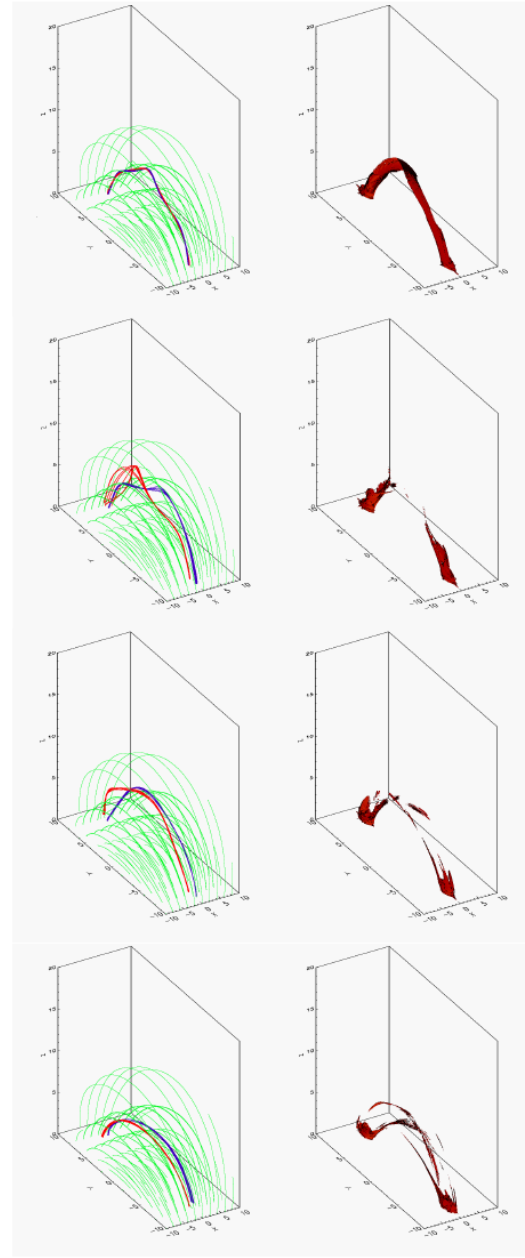
Above footpoints



Strongly-converging loop

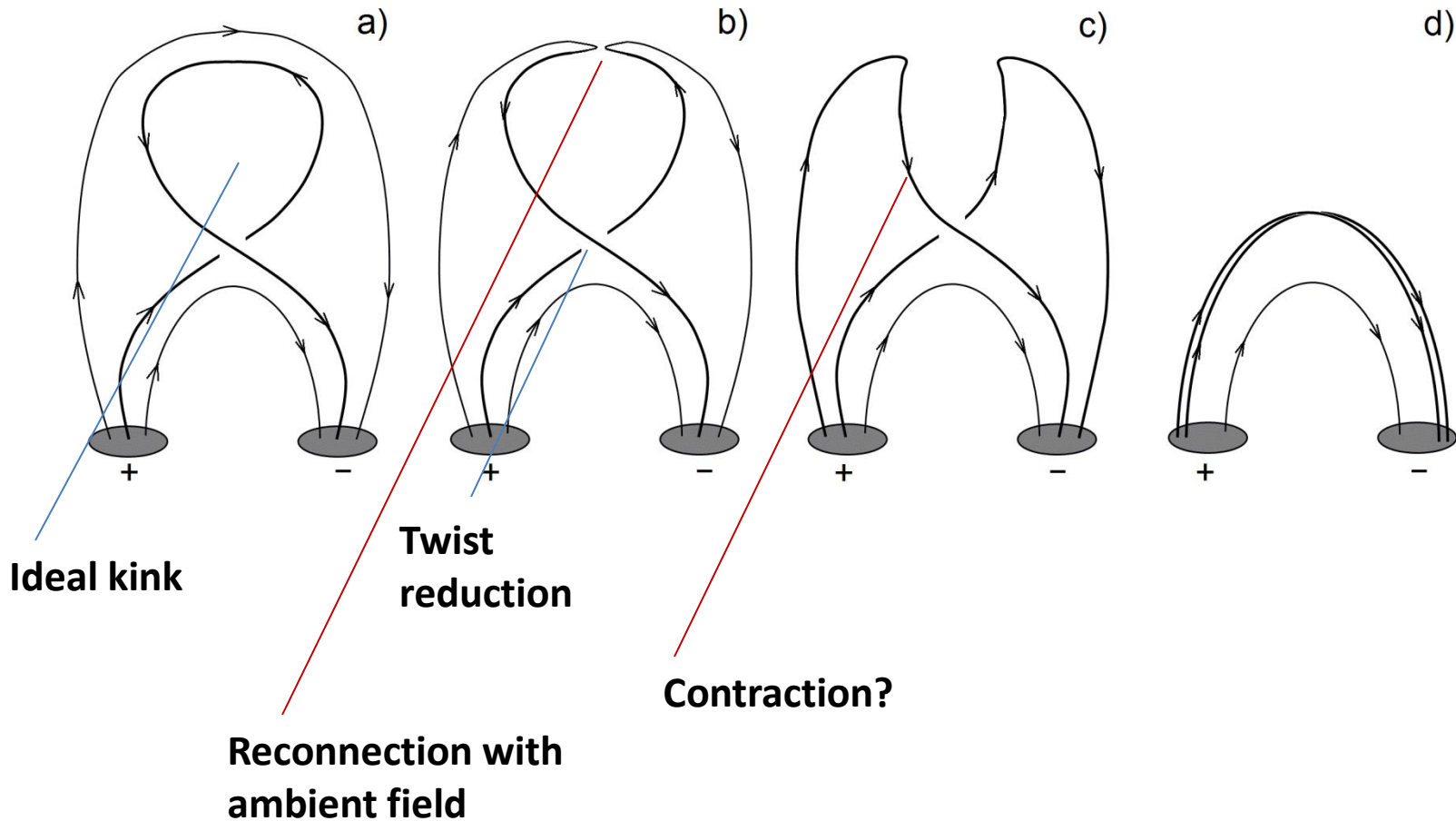


Weakly-converging loop



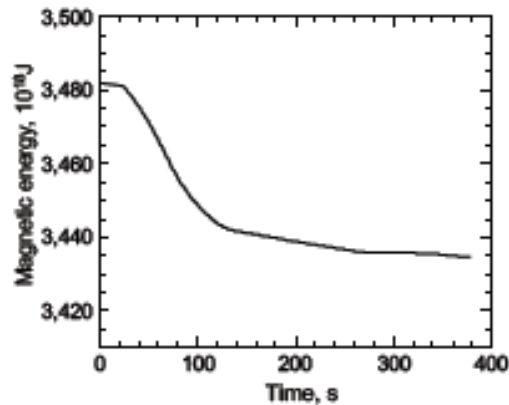
Curved loop – topology evolution

- Change of connectivity during magnetic reconnection in twisted loop

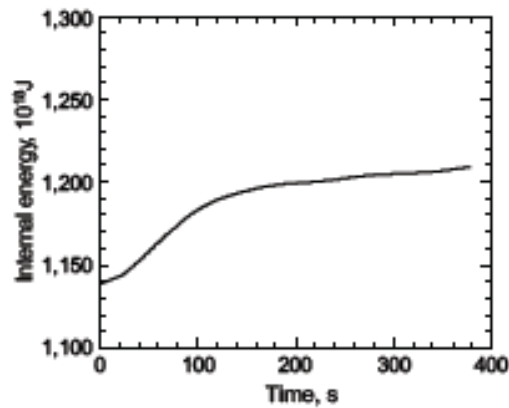


- Overlaying field prevents eruption (see also Torok & Kliem 2005)

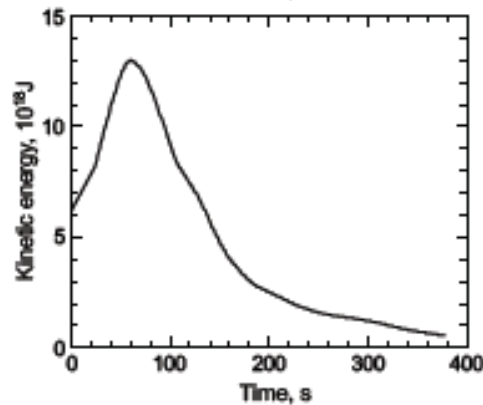
Energy release and heating



Magnetic
energy



Internal
energy



Kinetic
energy

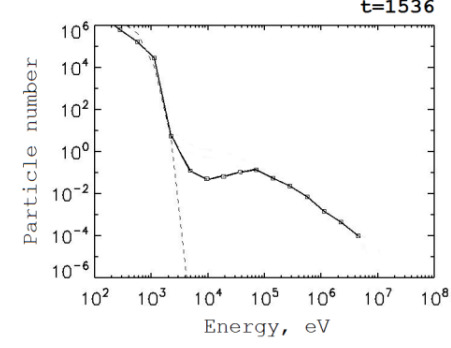
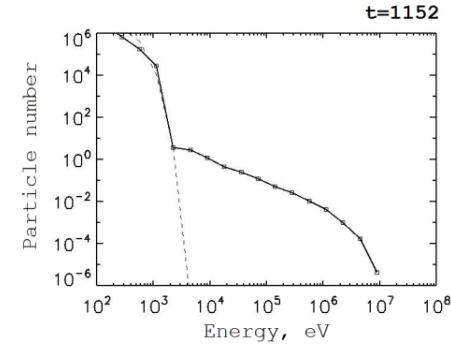
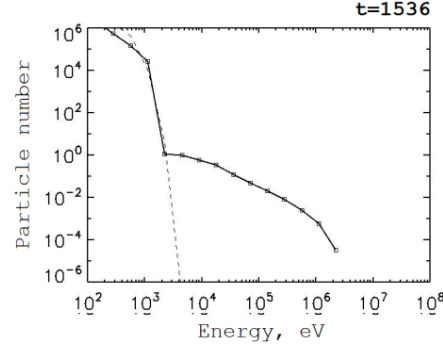
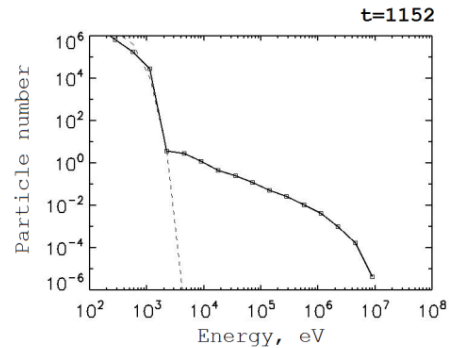
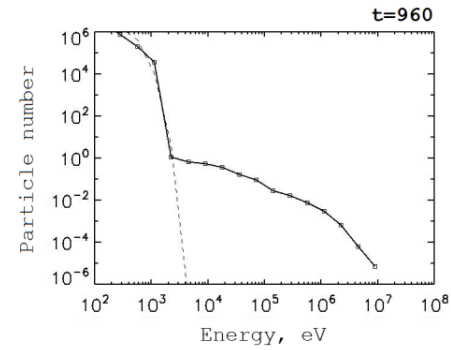
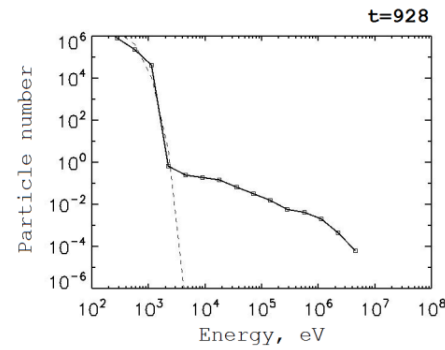
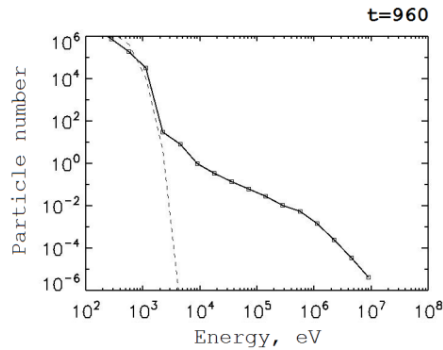
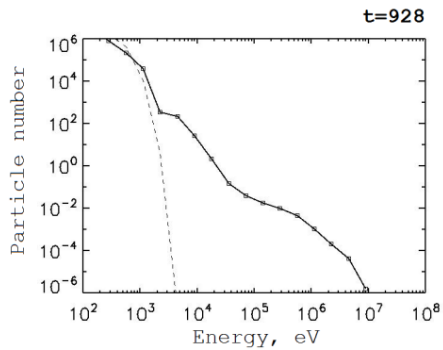
Time from
onset of
instability

Particle energy spectra – curved loop

Time evolution - electrons

Low density

High density



Gordovskyy et al 2014

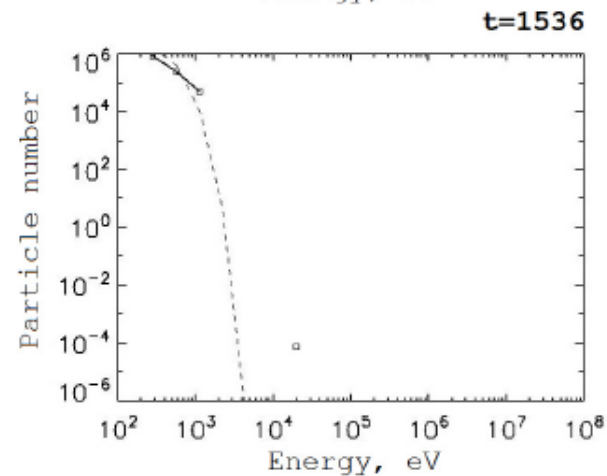
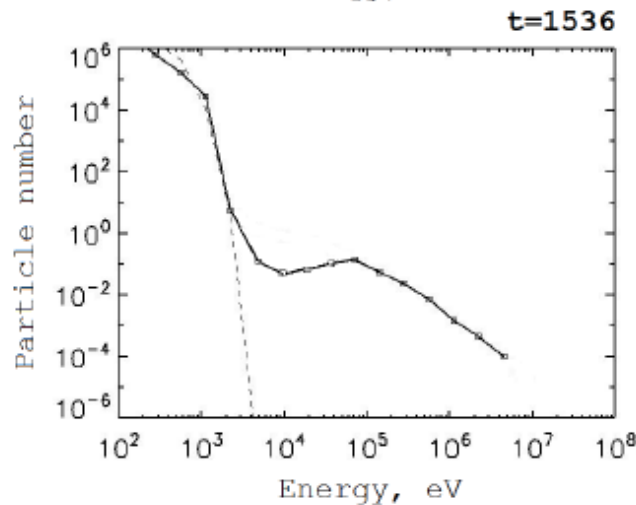
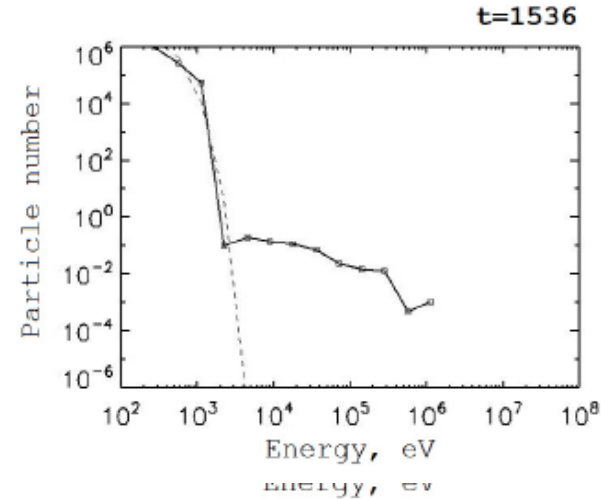
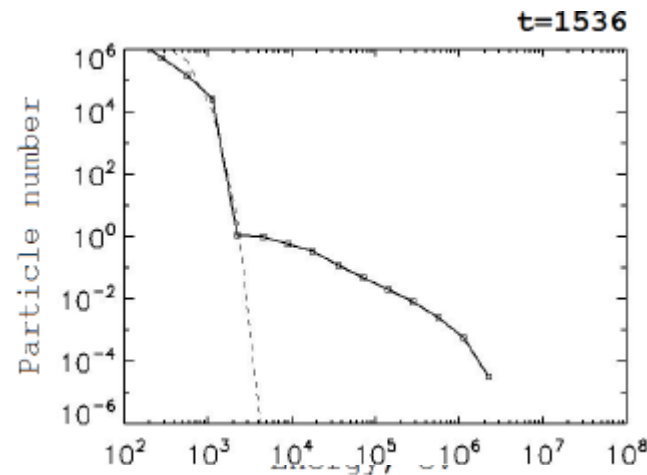
MHD without density stratification

Particle energy spectra – curved loop

Towards end of reconnection

Electrons

Protons

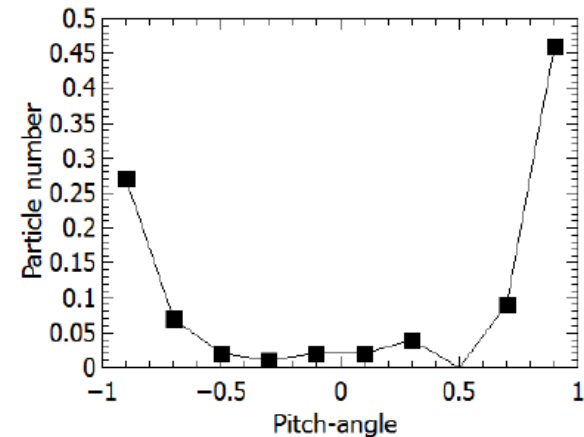
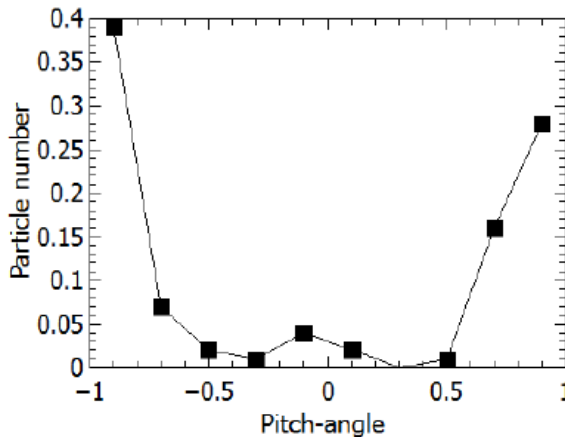


Gordovskyy et al 2014

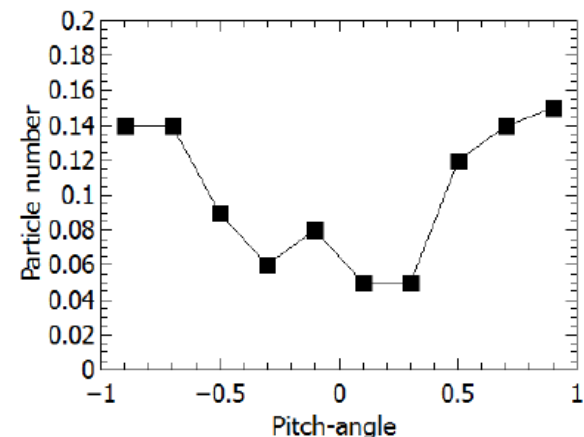
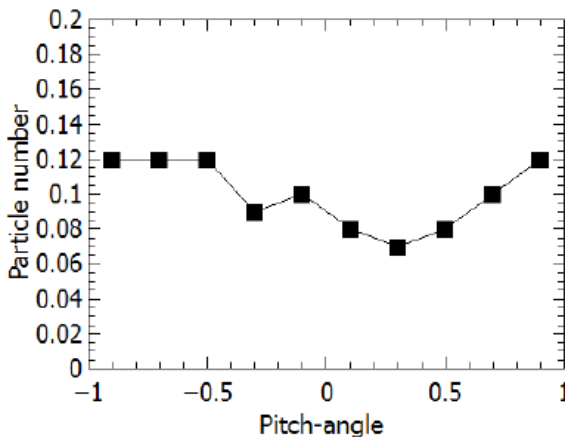
MHD without density stratification

Pitch angle distributions during main reconnection phase

Low density



High density



DC electric fields create strong anisotropic pitch angle distributions – mainly parallel

Electrons

Protons

MHD without density stratification

Gordovsky et al 2014

Acceleration efficiency

	Low-density model	High-density model
Electrons	7%	4%
Protons	6%	1%

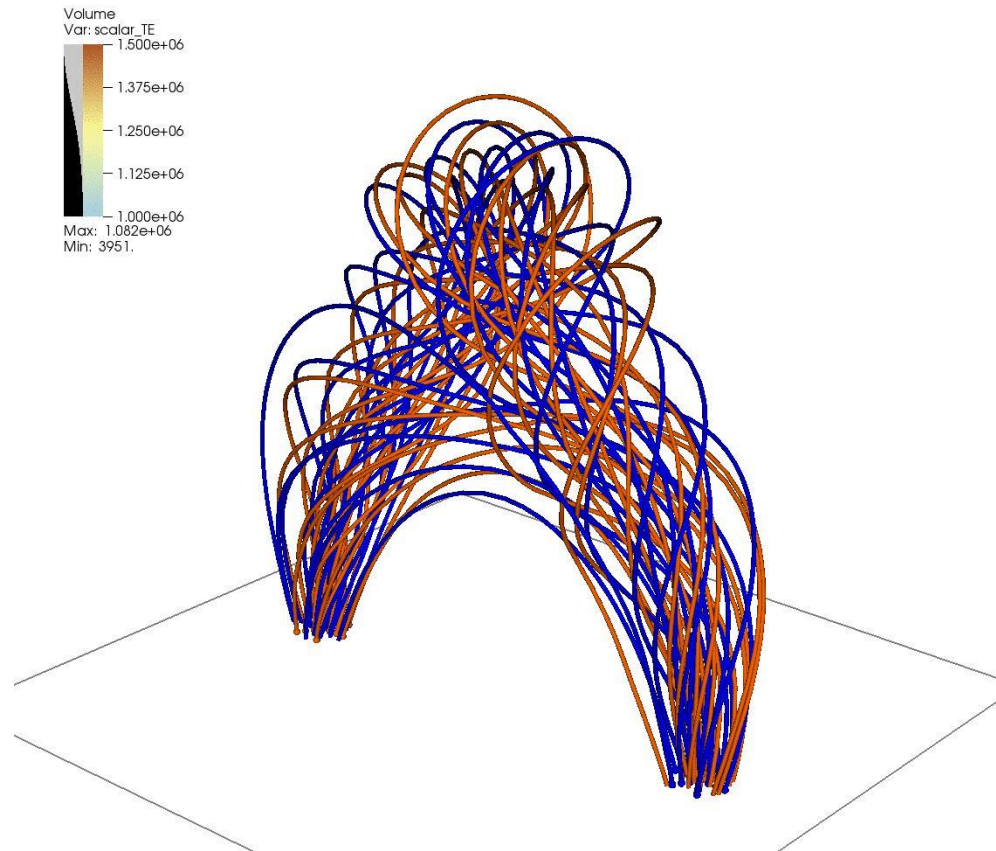
- Small fraction of particles accelerated (to > 1 keV) – validates use of test particles
- Energy transferred to non-thermal ions/electrons around 6-8% of released magnetic energy (low density model)
- Protons more strongly affected by collisions (for same energy) – proton acceleration suppressed in high-density loop

Gordovsky et al 2014

MHD without density stratification

Temperature distribution

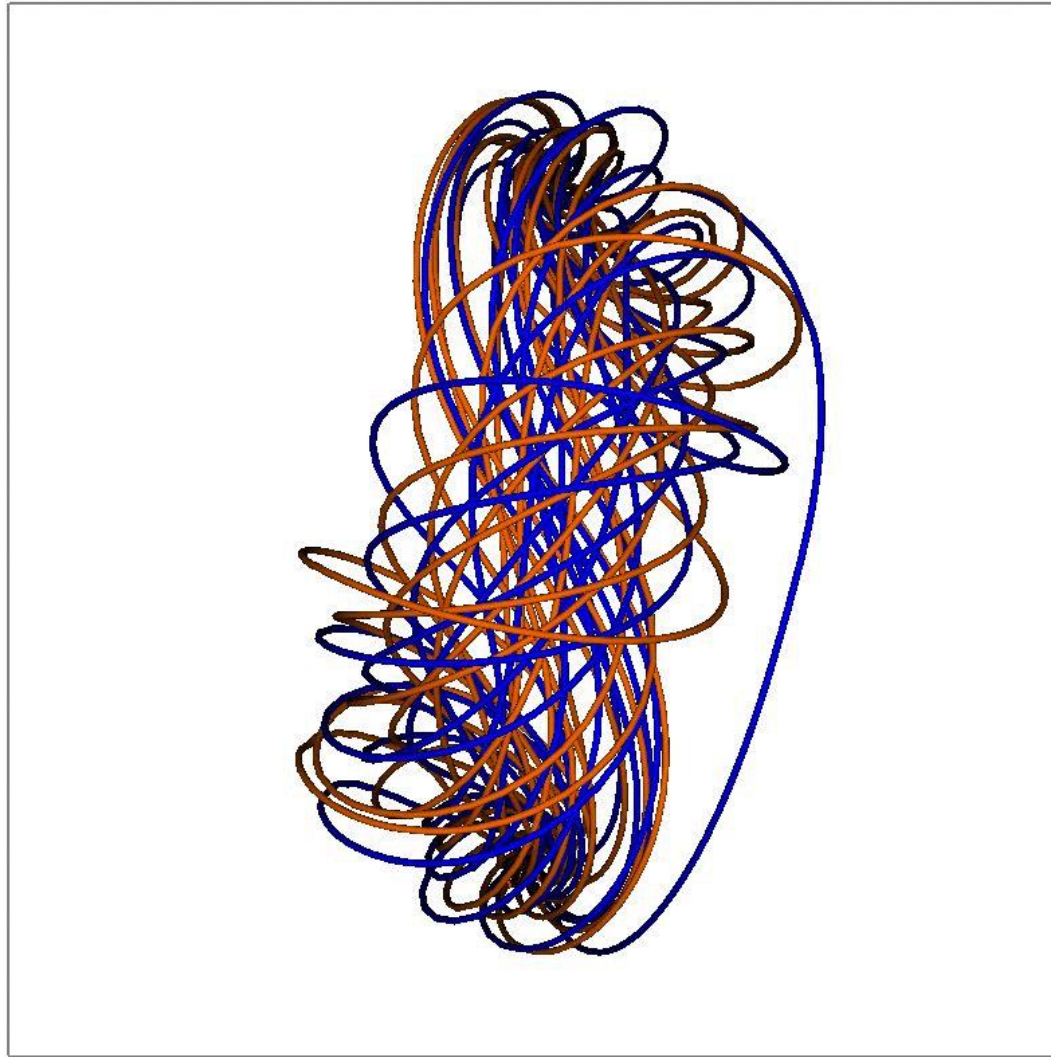
DB: experiment-s



Pinto, Gordovskyy, Browning and Vilmer

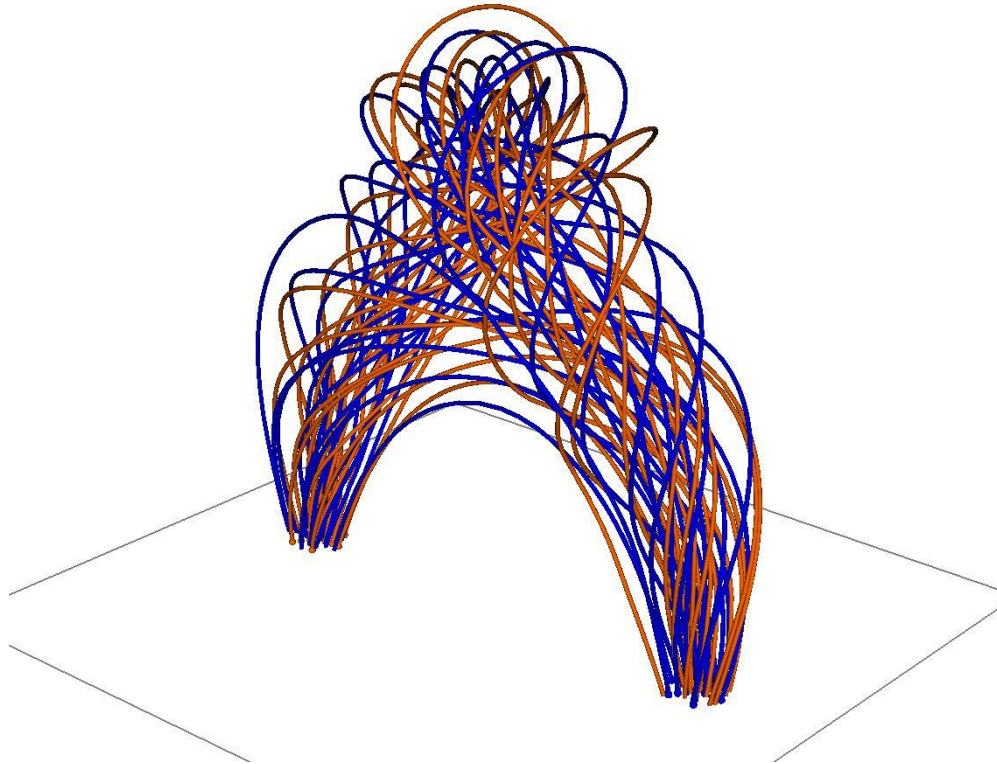
DB: experiment-s

Temperature distribution



Synthesised thermal emission

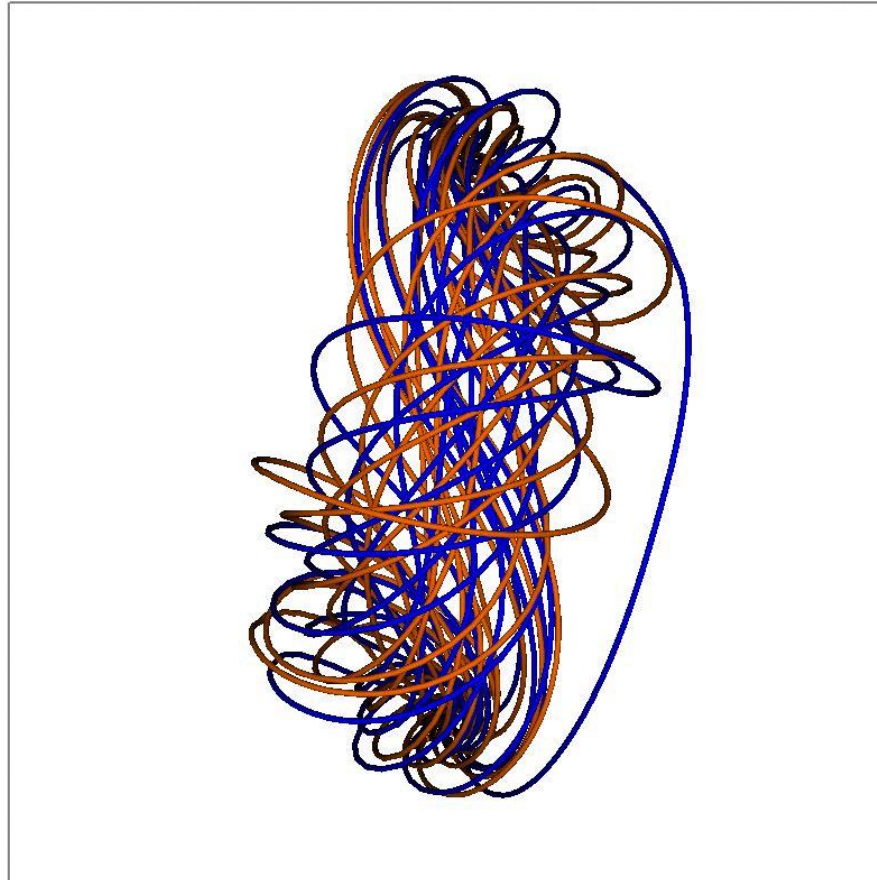
DB: experiment-s



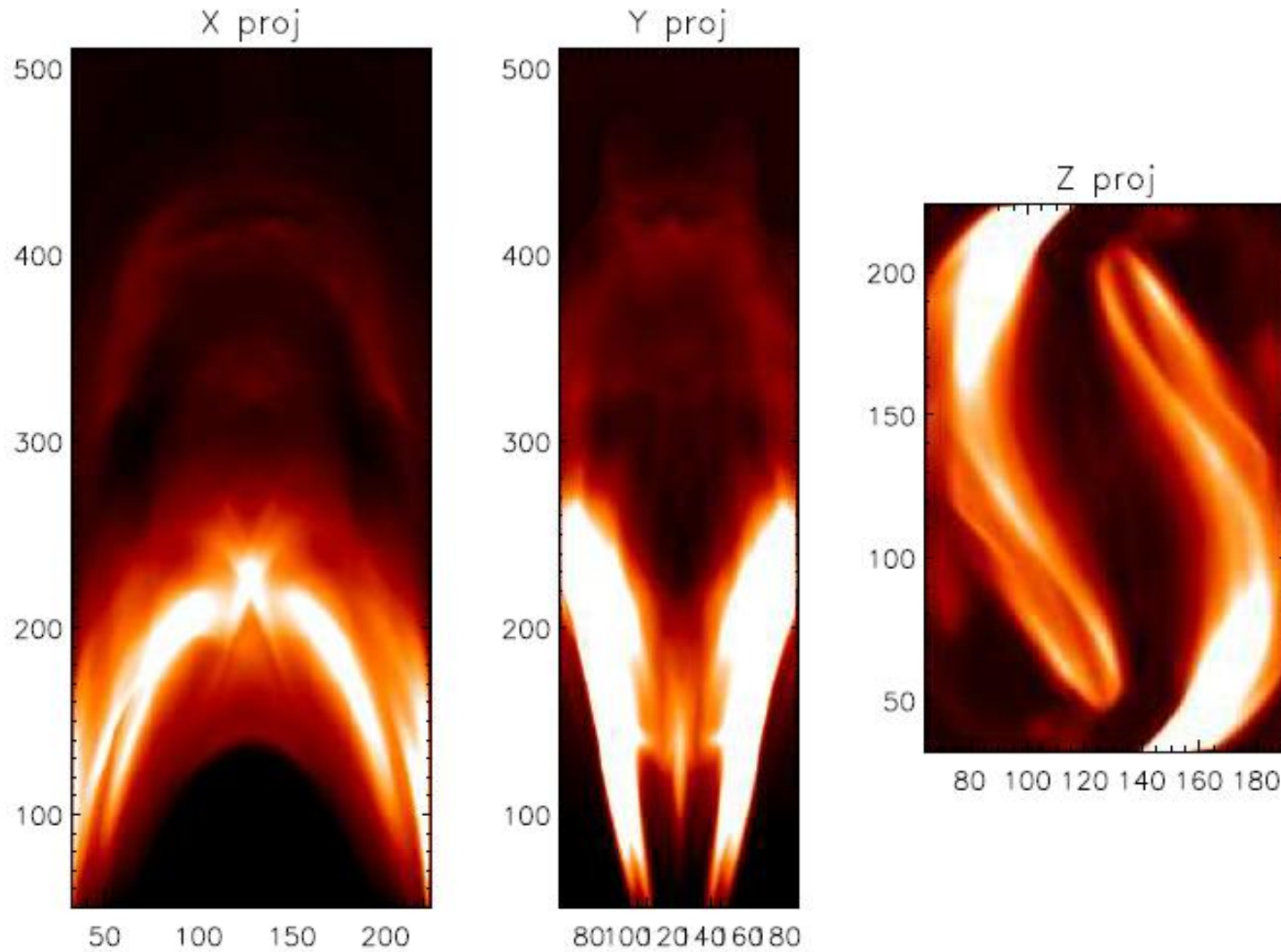
- 2 keV continuum emission
- Structures in emission are not strongly twisted despite highly-twisted initial magnetic field → we do not expect often to “see” twist

Synthesised thermal emission

DB: experiment-s

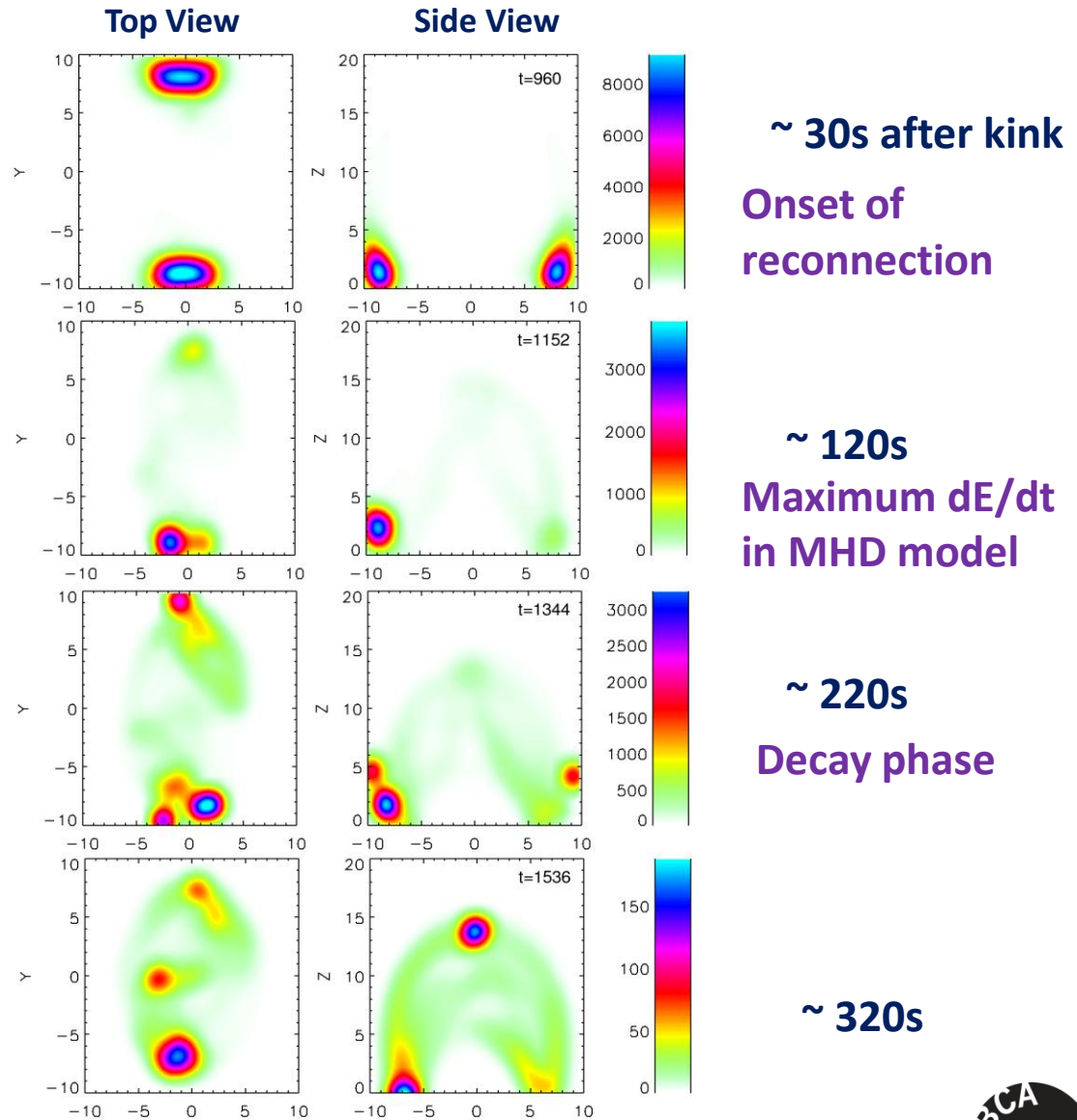


Synthesised thermal emission - image



Energetic particles and Hard X-ray emission

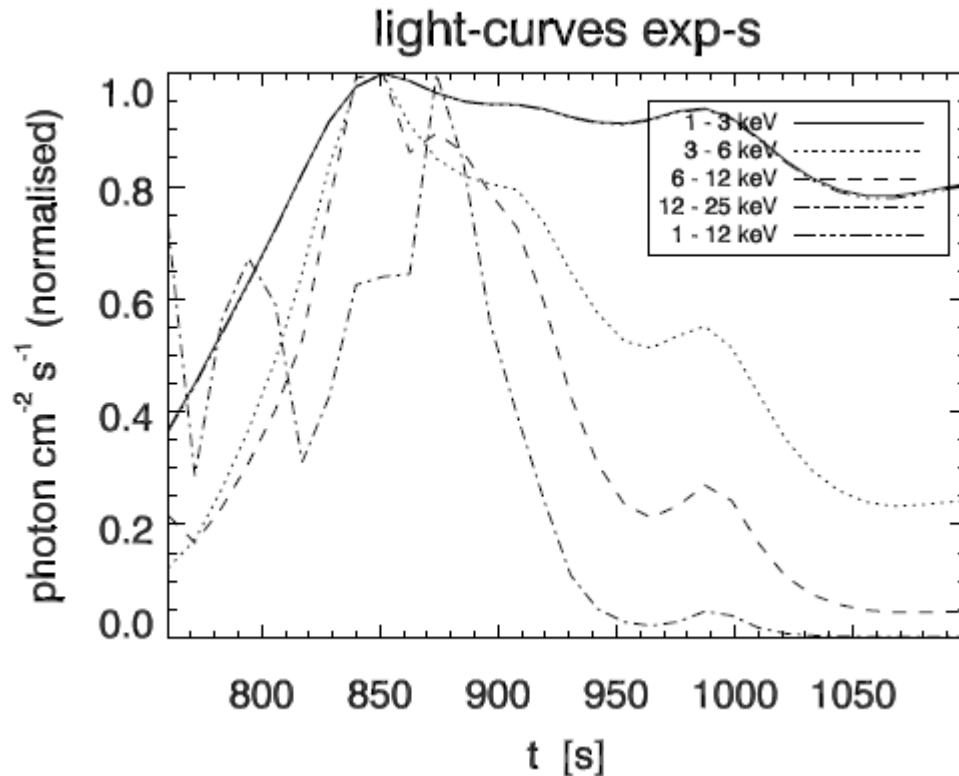
- Synthesise spatial and temporal dependence of Hard X-ray emission, compare with RHESSI observations



Synthesised HXR $\epsilon=10\text{keV}$

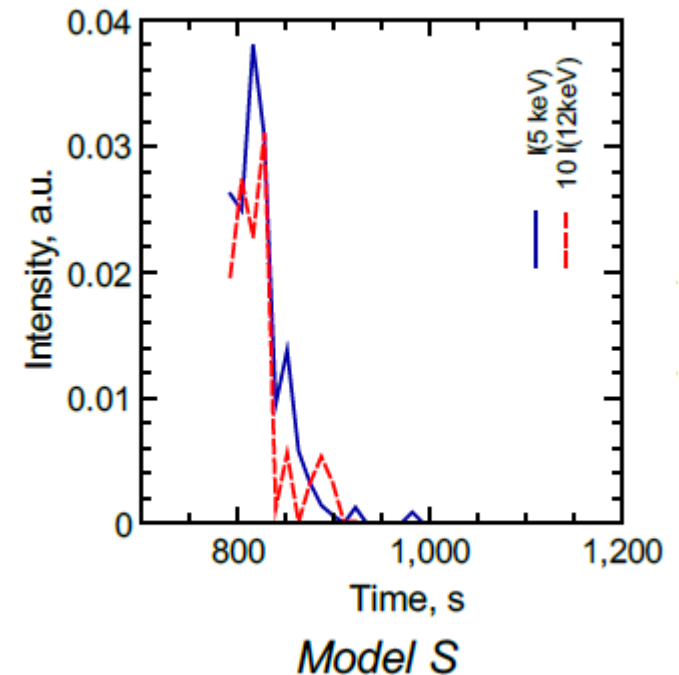
Gordovsky et al 2014

Synthesised light curves



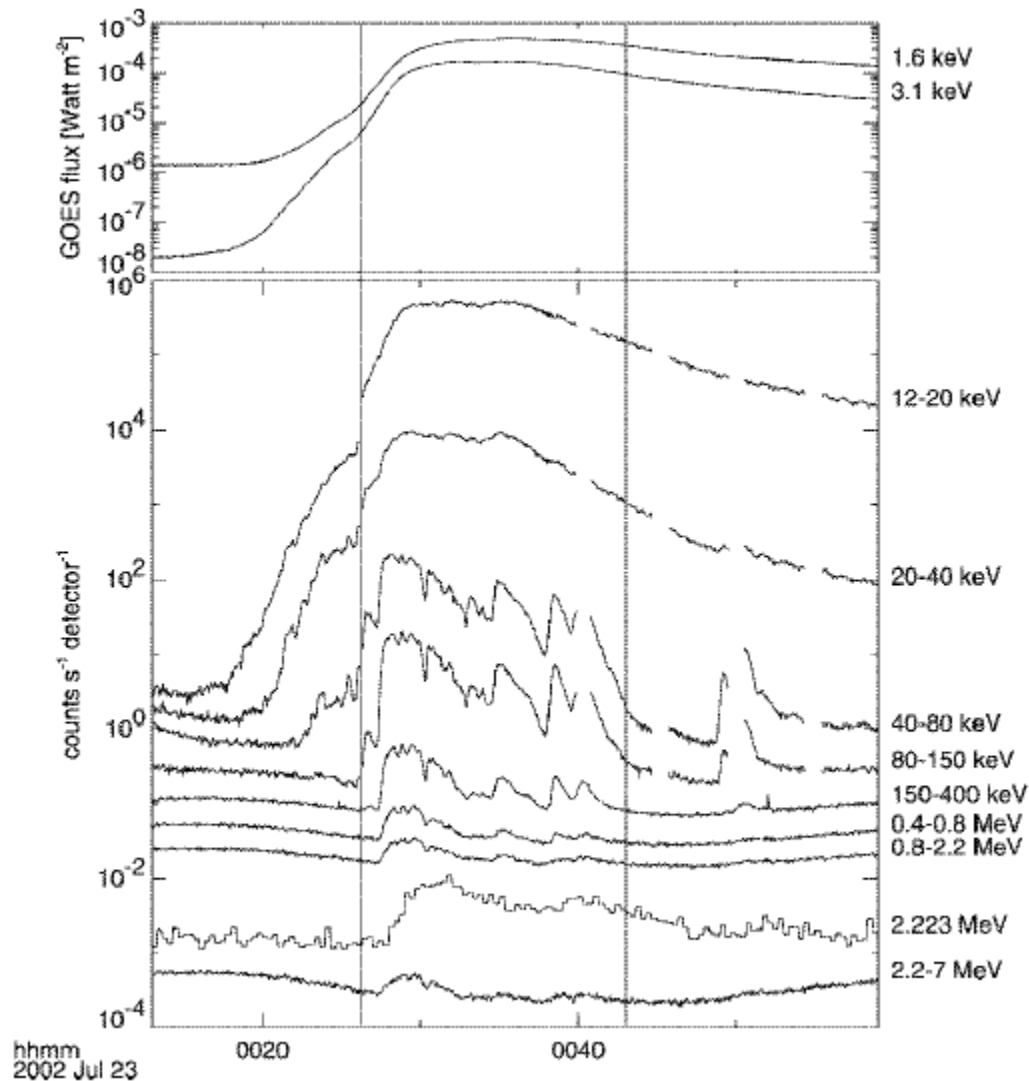
Thermal emission “Soft X rays”- different energy bands

Note higher energy bands shorter duration and “spikier”



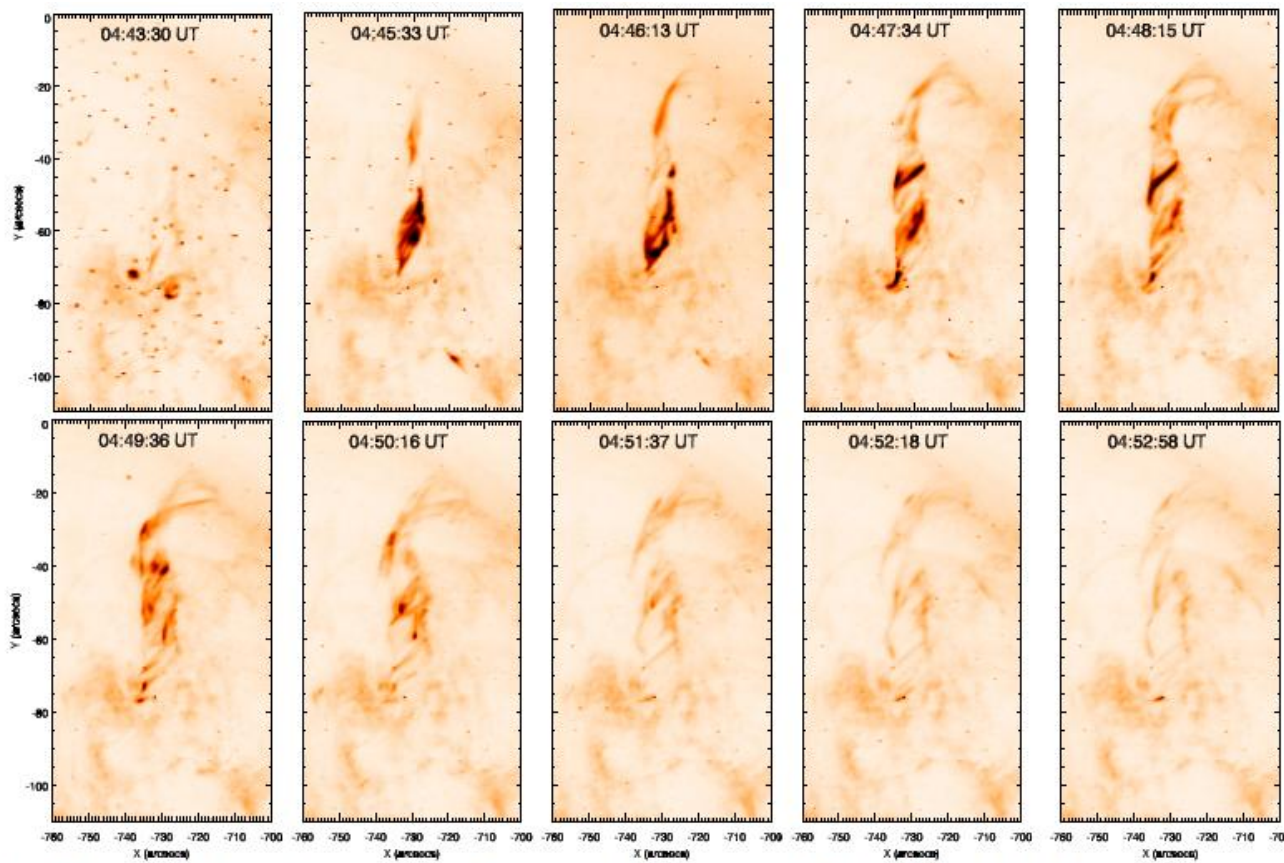
Non-thermal emission “Hard X rays”

RHESSI light curves



(For
much
larger
flare!)

Lin et al
2003



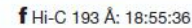
*Srivastava, et al.
2010, ApJ*

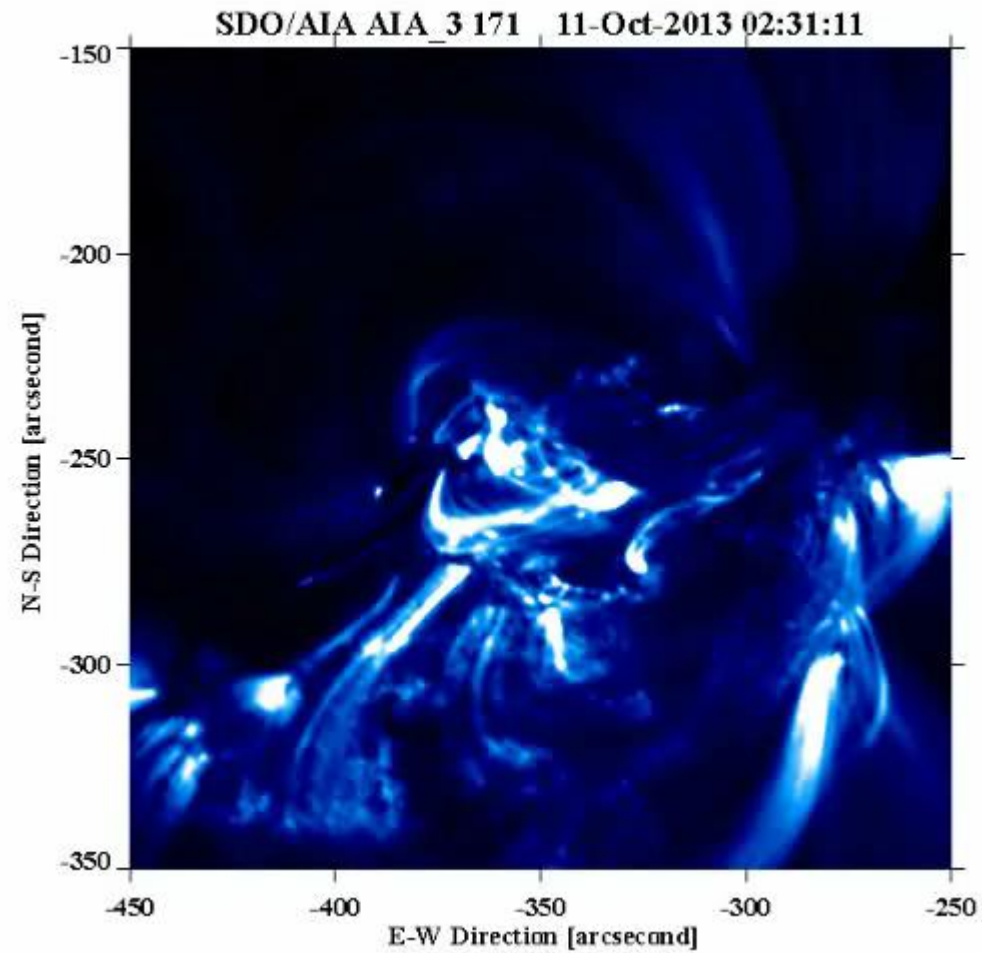
Figure 5. Time sequence of TRACE 171 Å Fe IX images of flaring loop in the AR 10960 during 04:43 UT–04:52 UT on 2007 June 4. The images are in reverse color and show the clear helical twist of the loop during the B5.0 flare. Note the double structure of the coronal loop top between 04:47 UT and 04:51 UT near $(X,Y) = (-720, -20)$.

- Compact self-contained flare
- Kink instability in the strongly twisted loop?

See also e.g. Liu et al 2013, Song et al 2014, Yan et al 2014

- Cirtain et al 2013***





**SDO video thanks to
Yan Xu**

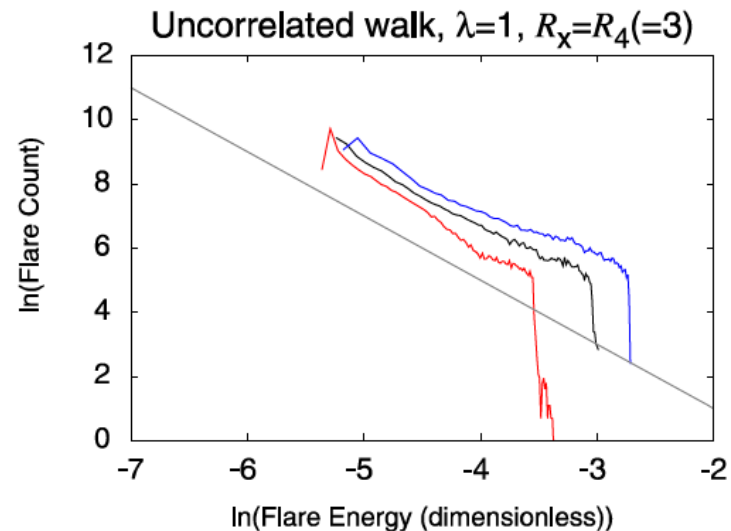
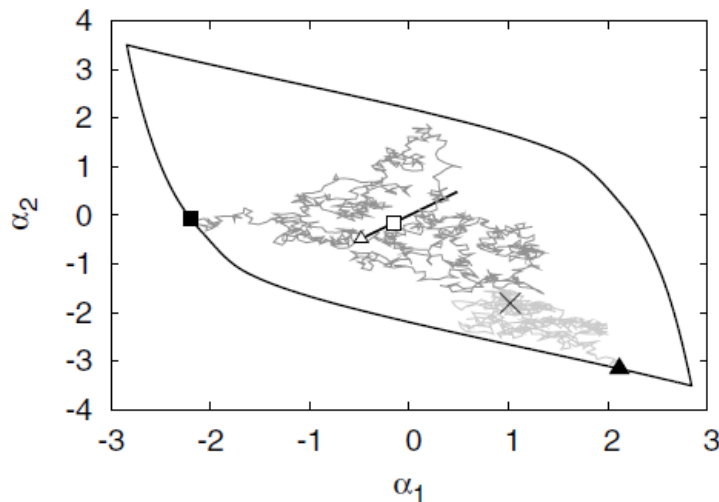
Beyond the single loop model

- Repeated heating events and multiple loops**
- Towards complex topologies**

Distributions of heating events and nanoflares

- Using relaxation theory, may evaluate energy released as heat for a wide range of initial current profiles, marginally-unstable to ideal kink
- Random photospheric footpoint motions generate range of current profiles - family of analytical models parameterised by piecewise constant $\alpha(r)$
- Energy release depends on current profile at onset of ideal instability
- Repeat many times, building distribution of heating events

Bareford et al 2010, 2011



Implications for coronal heating

- Estimate Poynting flux of energy from photosphere to corona

$$F = |\mathbf{E} \times \mathbf{B} / \mu_0| = B_v B_h v_{phot} / \mu_0$$

$$B_v \approx 100 \text{ G}, v_{phot} \approx 1 \text{ km s}^{-1}$$

where B_v and B_h are vertical/horizontal magnetic field

- In order to match required coronal heating flux, require sufficiently large B_h i.e must be sufficient stored free energy for effective heating

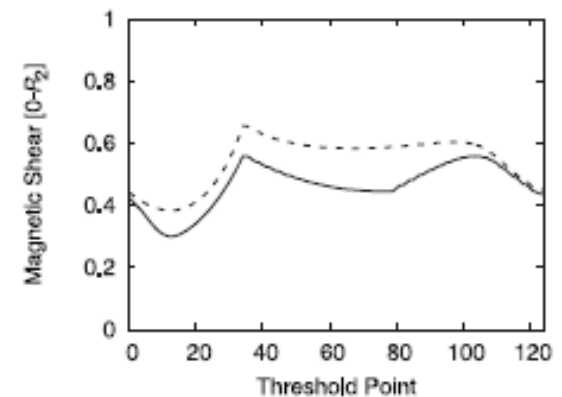
Parker 1983

- For relaxation nanoflare model, estimated heating flux is

$$F \approx \frac{81\pi}{2\mu_0} R_c B_c^2 \frac{\langle \delta W^* \rangle}{N\tau} \approx 3 \times 10^7 \text{ erg cm}^{-2} \text{ s}^{-1}$$

adequate for Active Region Heating

- Model predicts shear angle $B_h / B_v \approx 0.4$
matching above requirement

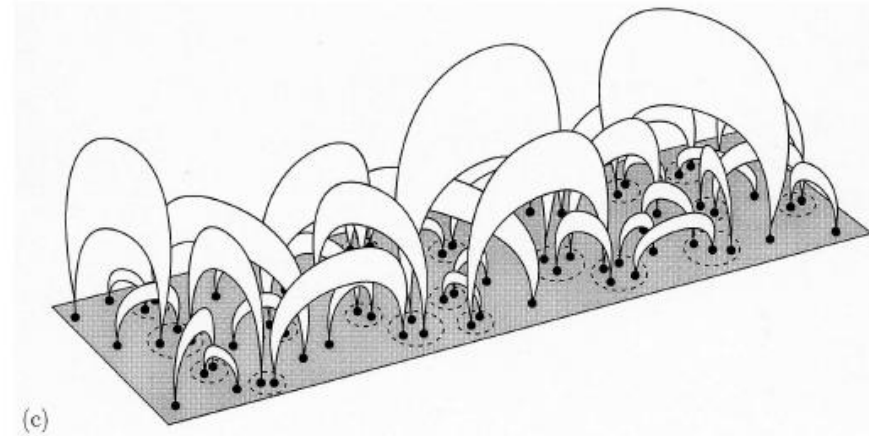


From Bareford et al 2010



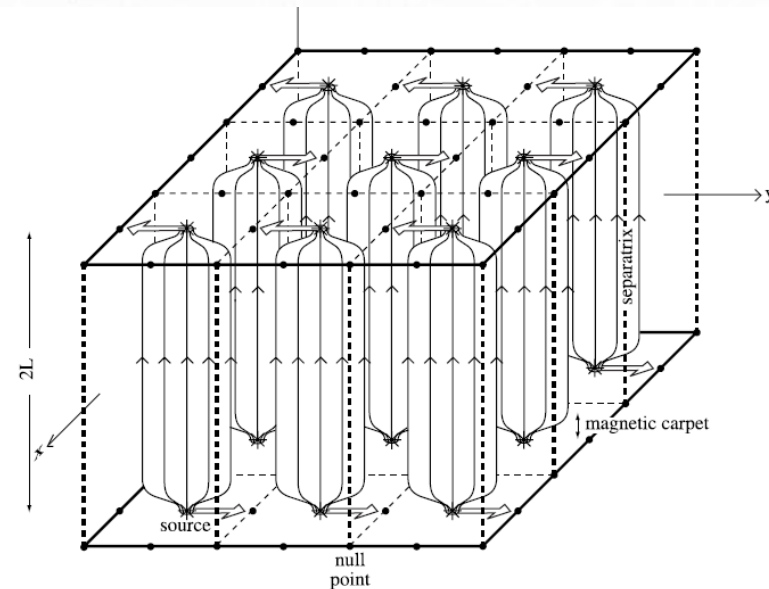
Interacting coronal loops – multi-thread structures

- Coronal loops may contain multiple threads
- Either due to discrete photospheric flux sources – flux tube tectonics (*Priest et al 2002*) or due to complex pattern of photospheric motions “braiding” within a single flux tube



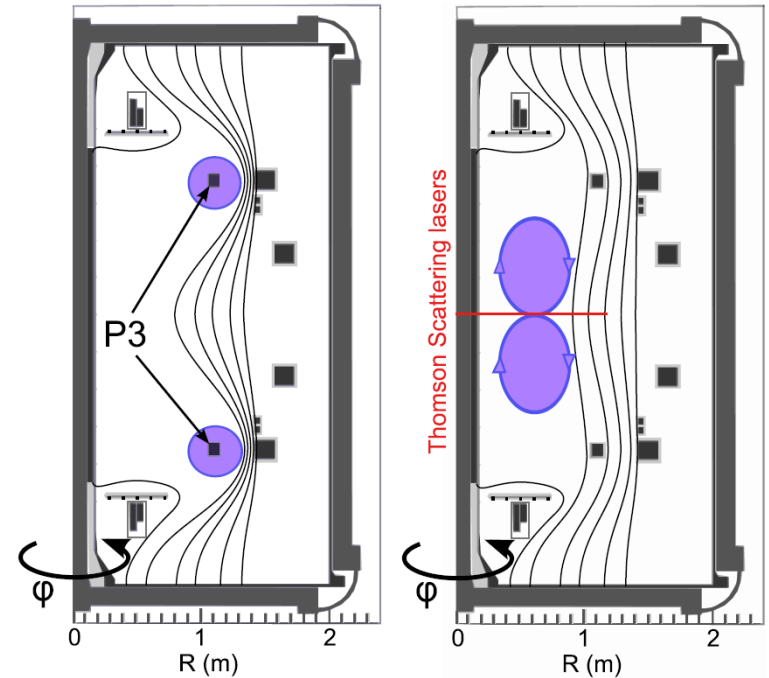
Consider here:

- Merging of two or more flux ropes carrying net current
- Destabilisation of one (or more) flux rope by a kink-unstable neighbour – potentially leading to an avalanche
- Repeated heating events with random driving



Merging-compression startup in MAST

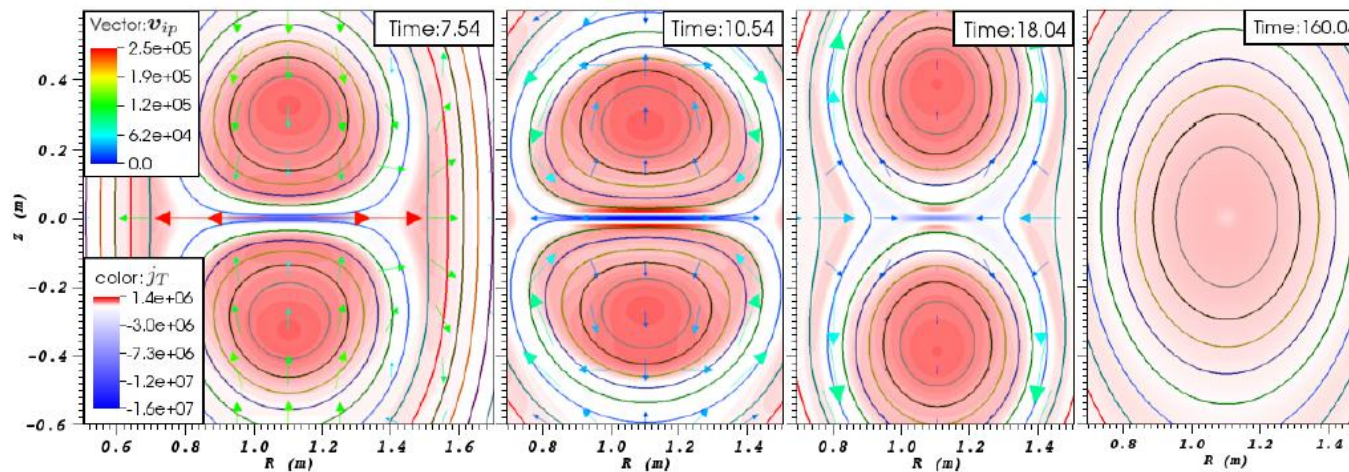
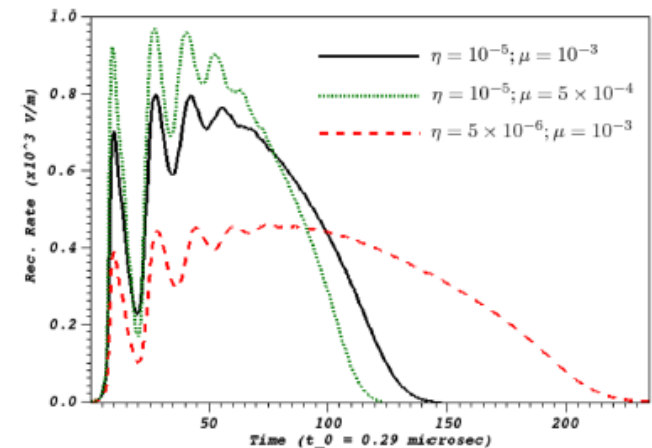
- One of several plasma start-up methods used in MAST spherical tokamak was merging-compression:
 - Two plasma rings “flux ropes” with parallel current attract & merge, forming plasma torus with single set of closed flux surfaces



Opportunity to study magnetic reconnection in well-diagnosed high temperature plasma with strong guide field - similar parameter regime to solar corona

Merging of two twisted flux ropes

- Consider two identical adjacent twisted flux ropes carrying net current
- These attract – current sheet is formed at interface due to reversing azimuthal field component
- Subsequently reconnect, forming a single twisted rope



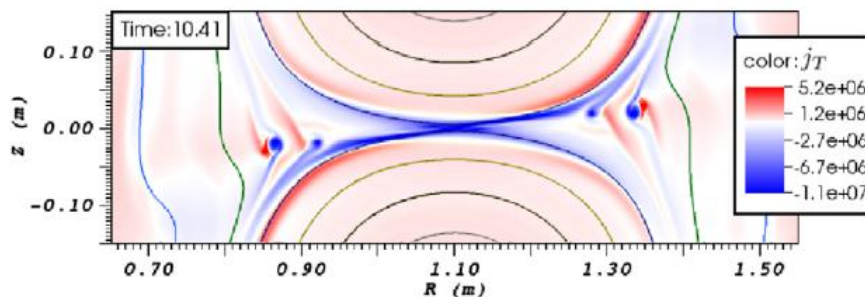
Resistive MHD simulation of two merging flux ropes in MAST spherical tokamak

*Stanier et al 2013,
Browning et al 2014*

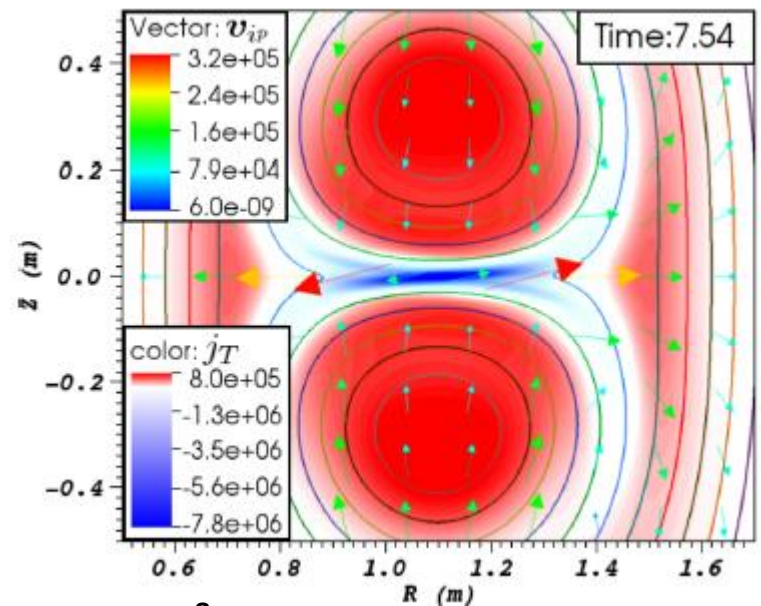
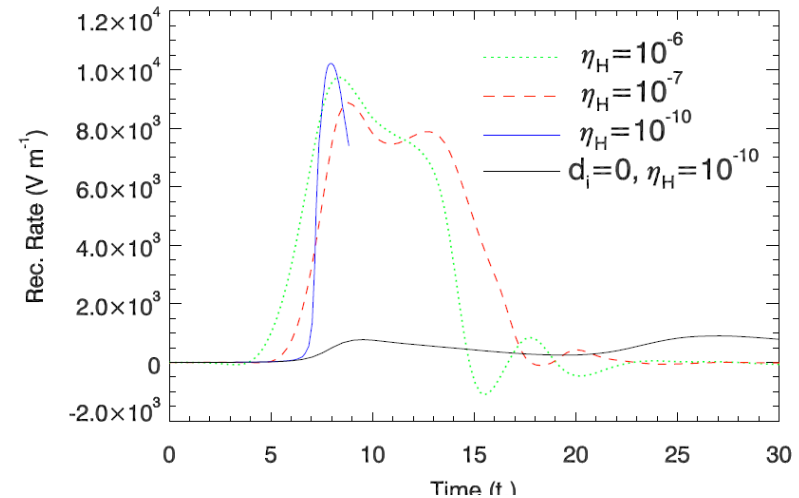
Hall MHD simulations of merging flux ropes

- Large ion skin depth in MAST plasmas
→ Hall MHD simulations (with hyper-resistivity)
- Hall MHD reconnection much faster than resistive MHD – peak reconnection rate insensitive to hyper-resistivity
- Current sheet tilts → asymmetric ion outflow jets
- At lower η_H current sheet fragments into series of islands

$$\eta_H = 10^{-9}$$



- At lowest values $\eta_H = 10^{-10}$ outflow opens leading to fast reconnection



$$\eta_H = 10^{-8}$$



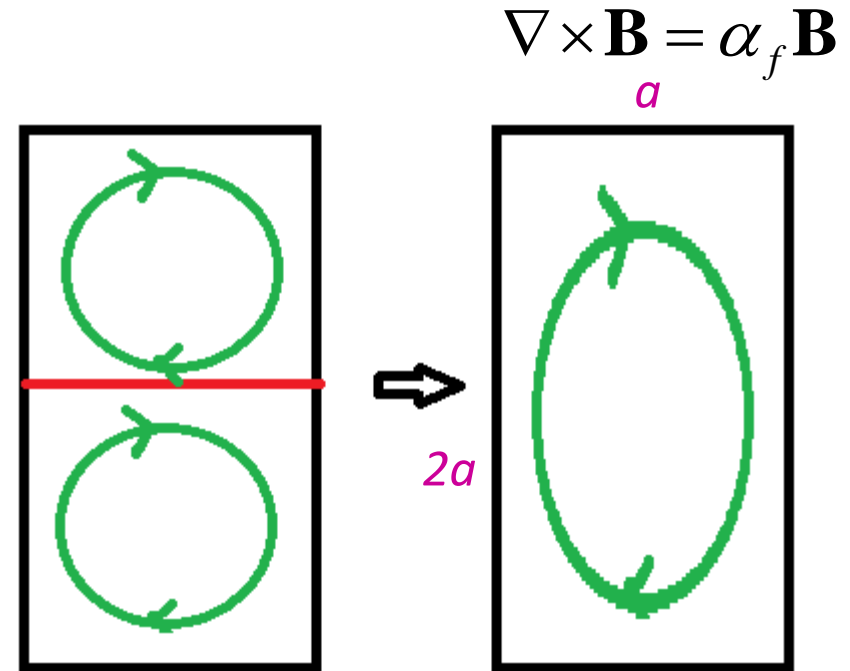
MAST merging and solar plasmas

Quantity	Solar flare	MAST merging-compression	<ul style="list-style-type: none"> • T_e, T_i & β values similar • Coronal S values are higher than those in MAST, but latter much higher than any other reconnection experiments • Predicted current sheet length scales in flares are comparable to ion skin depth – suggests that two-fluid effects should be taken into account when estimating reconnection rates in flares
<i>Typical values</i>			
Global length	$L \sim 10^7$ m	$L = 1$ m	
Ion species	Hydrogen	Deuterium	
Magnetic	$B \sim 0.01$ T	$B_p = 0.1$ T, $B_T = 0.5$ T	
Temperature	$T \sim 100$ eV	$T = 10\text{--}1000$ eV	
Density	$n \sim 10^{15}$ m ⁻³	$n = 5 \times 10^{18}$ m ⁻³	
<i>Dimensionless</i>			
Plasma- β	$\beta = 10^{-4}\text{--}10^{-2}$	$\beta_T = 10^{-4}\text{--}10^{-2}$, $\beta_p = 10^{-3}\text{--}10^{-1}$	
Lundquist number	$S = 10^{12}\text{--}14$	$S = 10^{4-7}$	
<i>Non-MHD</i>			
Ion skin-depth	$d_i = 10$ m	$d_i = 14.5$ cm	
Ion gyro-radius	$\rho_i = 0.1\text{--}1$ m	$\rho_i = 0.15\text{--}1.5$ cm	
<i>Current-sheet</i>			
Sweet–Parker width	$\delta_{SP} = 1\text{--}10$ m	$\delta_{SP} = 0.03\text{--}1$ cm	
δ_{SP}/d_i	0.1–1	0.002–0.07	

Relaxation model of merging flux ropes

Browning et al PPCF 2014

- Rectangular boundary $a \times 2a$
- Two initial identical flux ropes $a \times a$, each with linear force-free internal current profile, $\alpha = \alpha_i$ separated by current sheet
- Not minimum energy state due to current sheet
- Relaxation to a single flux rope $\alpha = \alpha_f$ determined by conservation of helicity and axial (toroidal) flux



$$\Phi_t = \int_A B_\phi dRdZ = \oint_b \mathbf{A} \cdot d\mathbf{r}$$

Taylor 1974

$$K = \int_V \mathbf{A} \cdot \mathbf{B} dV$$

Helicity conserved

- **Solution of Grad-Shafranov equation**

$$\frac{\partial^2 \psi}{\partial R^2} + \frac{\partial^2 \psi}{\partial Z^2} + \alpha^2 \psi = 0$$

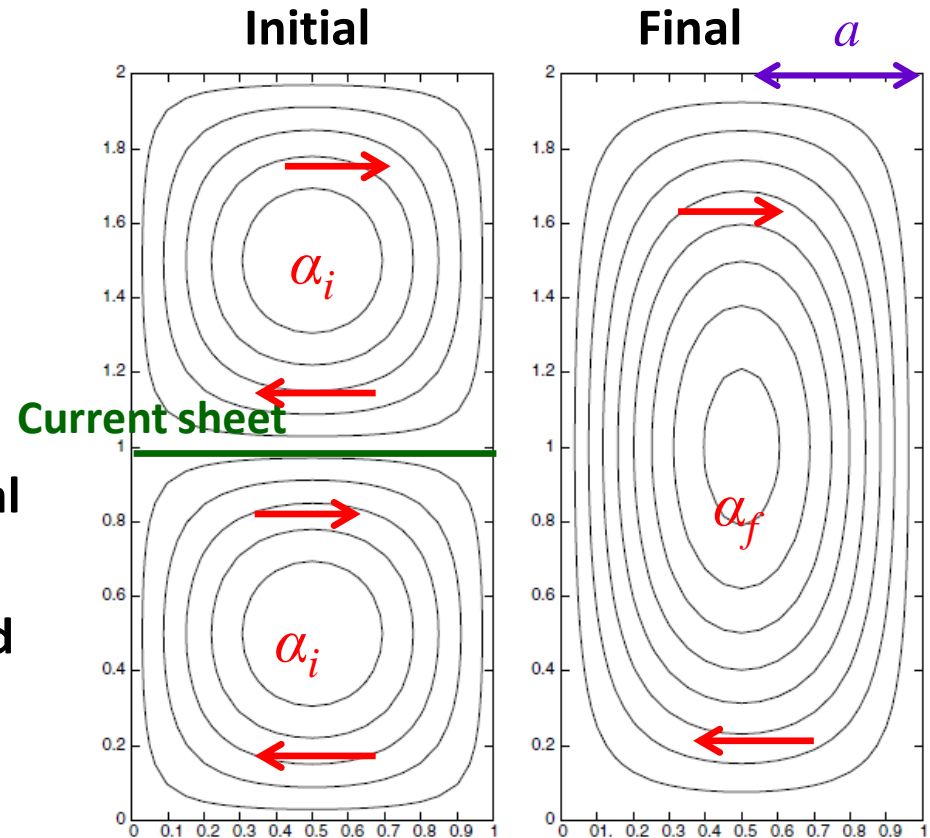
$$\psi = \psi_b \left[1 + \sum_{m,n} a_{mn} \sin\left(\frac{m\pi R}{a}\right) \sin\left(\frac{n\pi Z}{b}\right) \right]$$

where a_{mn} determined from GS equation using orthogonality

- For both initial field ($b = a$) and final field ($b = 2a$)
- Final α_f determined by helicity and flux conservation
- **Energy W**

$$W(\alpha; a, b) = \frac{ab\psi_b^2}{2\mu_0} \left[\alpha^2 + \sum_{m,n \text{ odd}} \left\{ \frac{a_{mn}^2}{4} \left(\frac{m^2 \pi^2}{a^2} + \frac{n^2 \pi^2}{b^2} + \alpha^2 \right) + \frac{8a_{mn} \alpha^2}{\pi^2 mn} \right\} \right]$$

Azimuthal field lines B_x B_y
Also axial field component B_z



Relaxation model of merging coronal flux ropes

- Dimensionless energy release/per unit length ΔW scales roughly quadratically with initial flux rope current α_i

$$\Delta W^* \approx 0.1(\alpha_i R)^2$$

- Estimate heating as

$$W_{heat} \approx 0.1 \frac{1}{\mu_0} \alpha_i^2 B^2 R^4 L$$

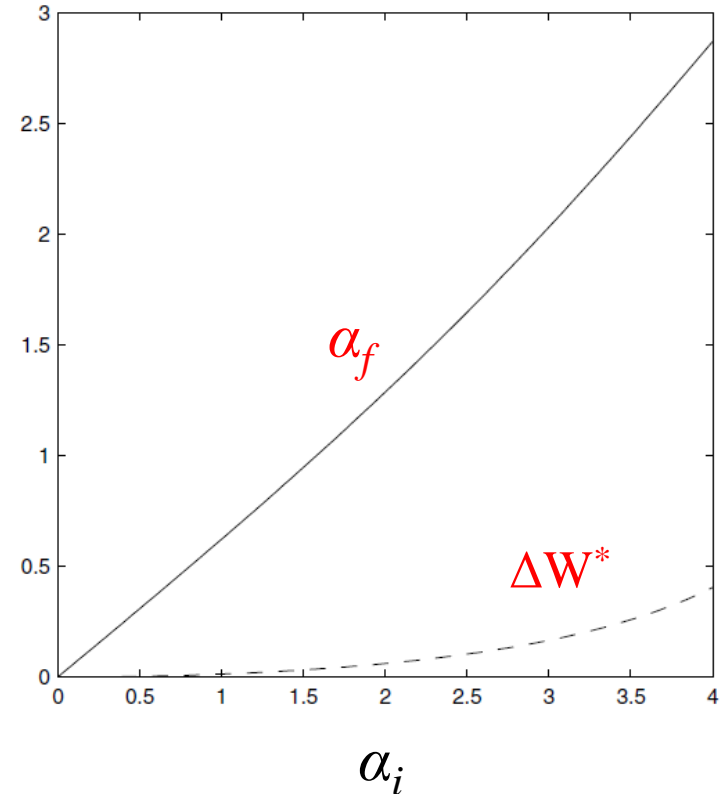
$$B = 0.01 \text{ T}, R = 1 \text{ Mm}, L = 10 \text{ Mm}$$

$$\alpha \approx 2\Phi/L \text{ - take weak twist } \Phi = \pi$$

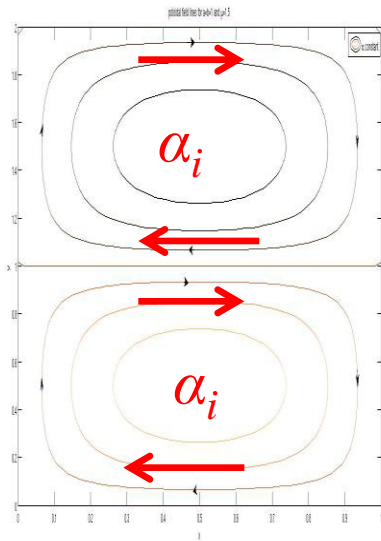
$$\Rightarrow W_{heat} \approx 10^{19} \text{ J}$$

- Gives average temperature rise ΔT

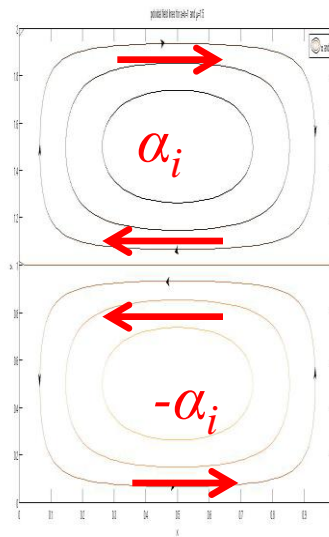
$$(4R^2 L) 2 \frac{3}{2} n k \Delta T = W_{heat} ; \text{ taking } n = 10^{15} \text{ m}^{-3} \Rightarrow \Delta T \approx 10^7 \text{ K}$$



Merging tubes – varying twist direction

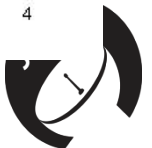
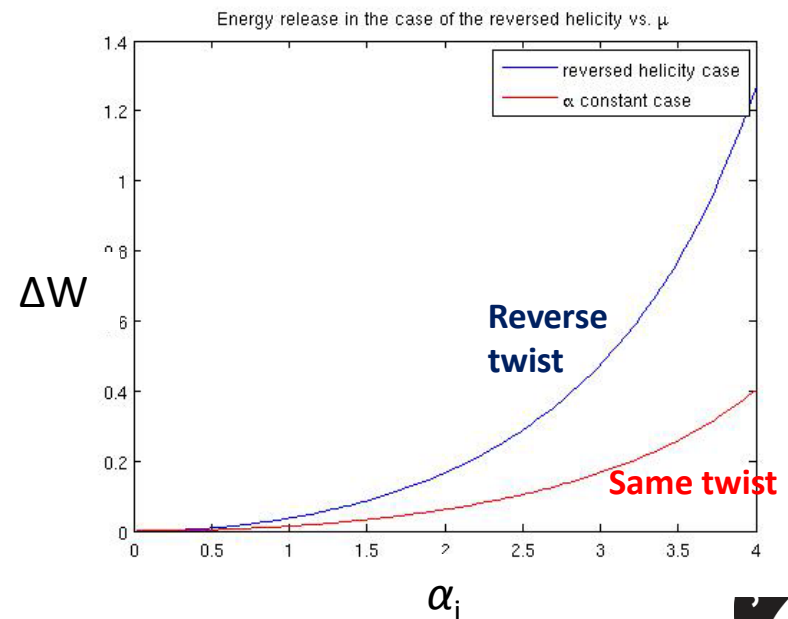


Same twist
“co-helicity”
 $\rightarrow \alpha = \alpha_f$



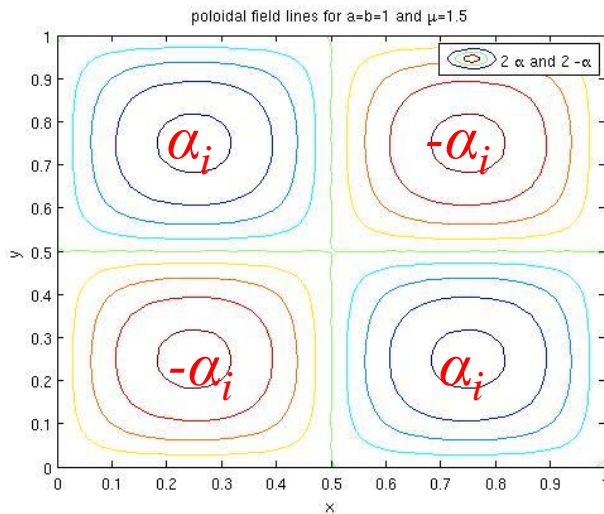
Reverse twist
“counter-helicity”
 $\rightarrow \alpha = 0$

- If loops have opposite twist but same axial field, reconnection is much less likely (unless strongly perturbed?) since azimuthal fields are parallel at interface
- But free energy is much greater since minimum energy state is potential

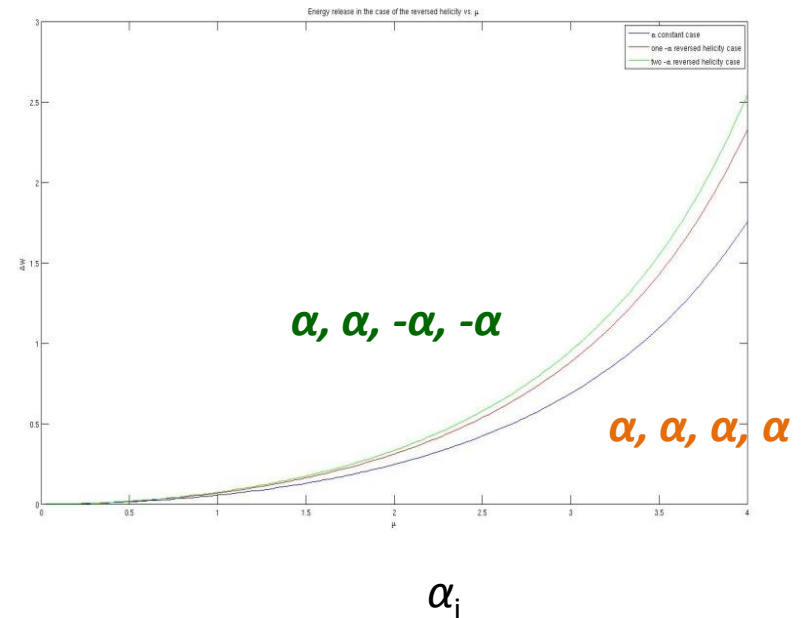


Relaxation of multiple merging coronal loops

- Consider n twisted loops merging
- May merge completely into single loop or partially (less energy release)



ΔW



$n = 4$ – consider all cases of equal/opposite twist:

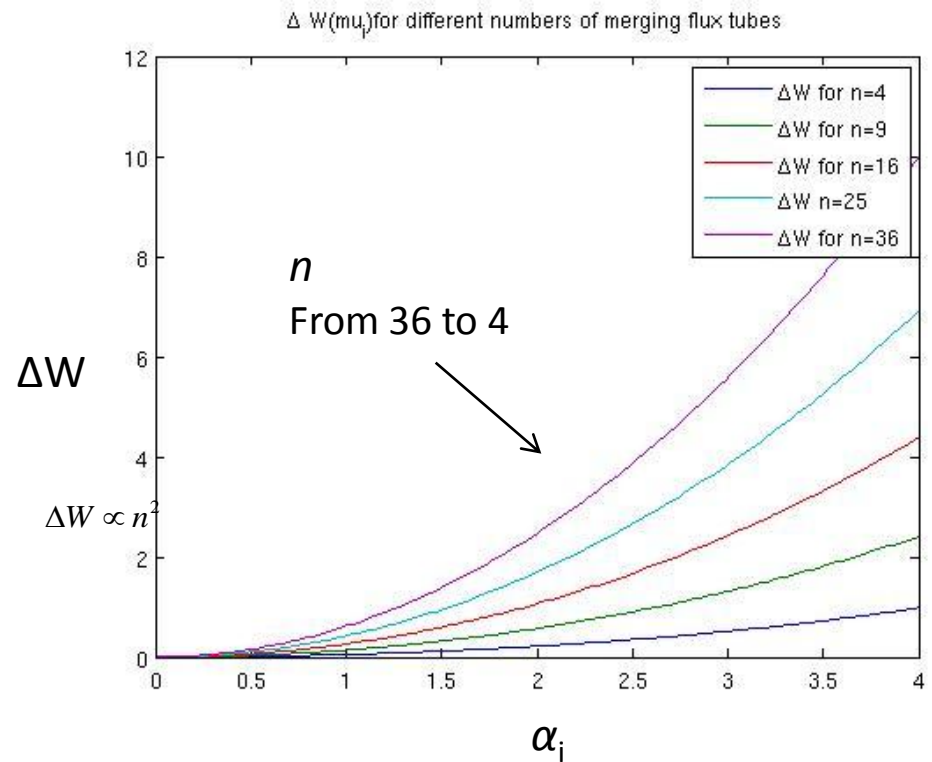
$\alpha, \alpha, \alpha, \alpha$ *Least energy release*

$\alpha, \alpha, \alpha, -\alpha$

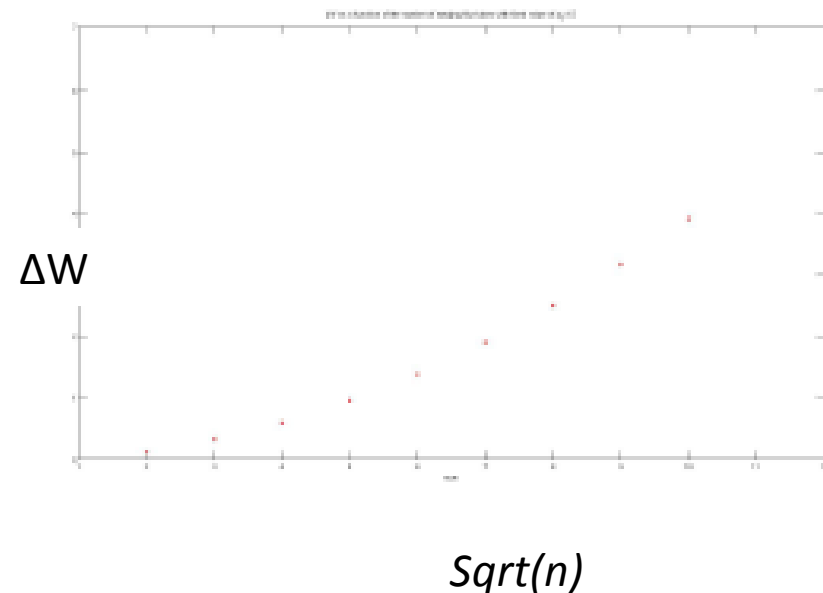
$\alpha, \alpha, -\alpha, -\alpha$ *Greatest energy release*

Multiple merging tubes

- Energy release is increases as number of flux tubes within a given volume increases
- Due to increasing number of current sheets



$$\Delta W \sim n$$



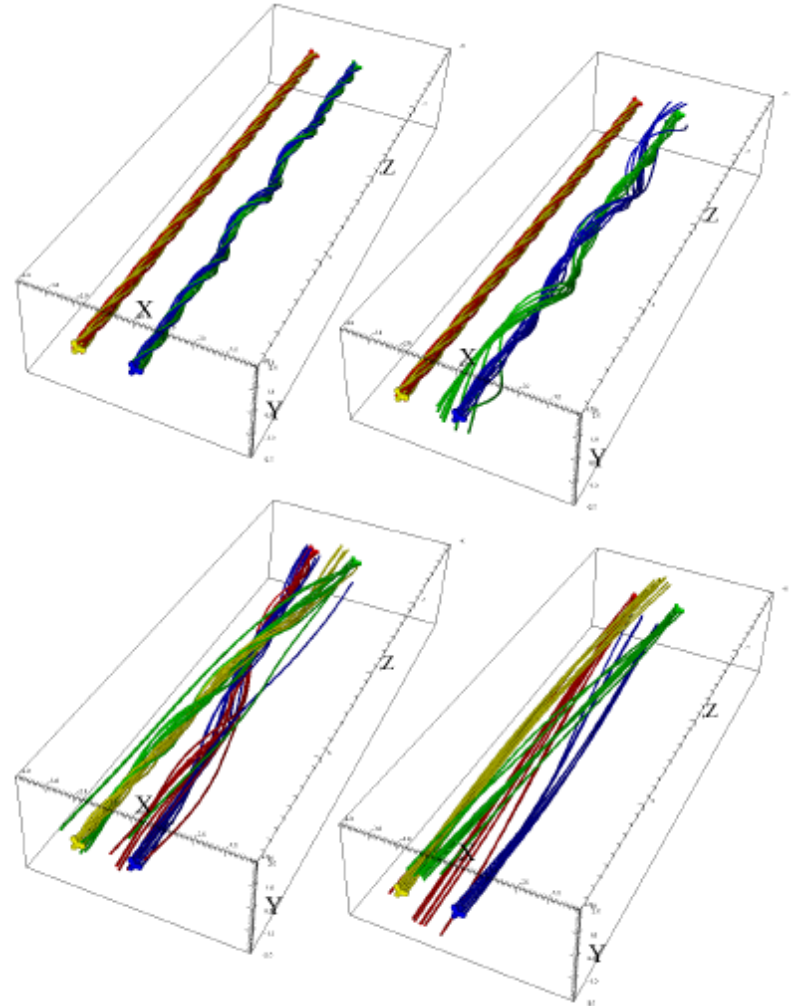
“Avalanche”- disruption of neighbouring stable loop

Tam, Hood, Browning and Cargill (in preparation) 2014

- Consider adjacent zero net current loops
- If the loops are sufficiently close, an unstable loop may trigger relaxation in a neighbouring stable loop
- In this case the two loops relax into a single (very weakly twisted) loop

→ Under certain conditions can have an avalanche of heating events

Cf Lu and Hamilton 1981, Charbonneau et al 2001



Stable
loop

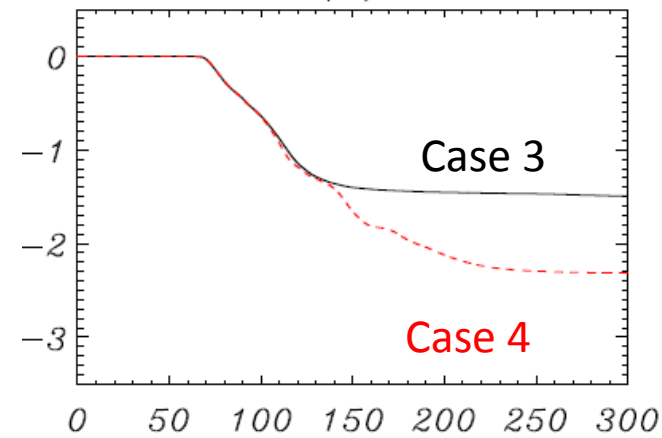
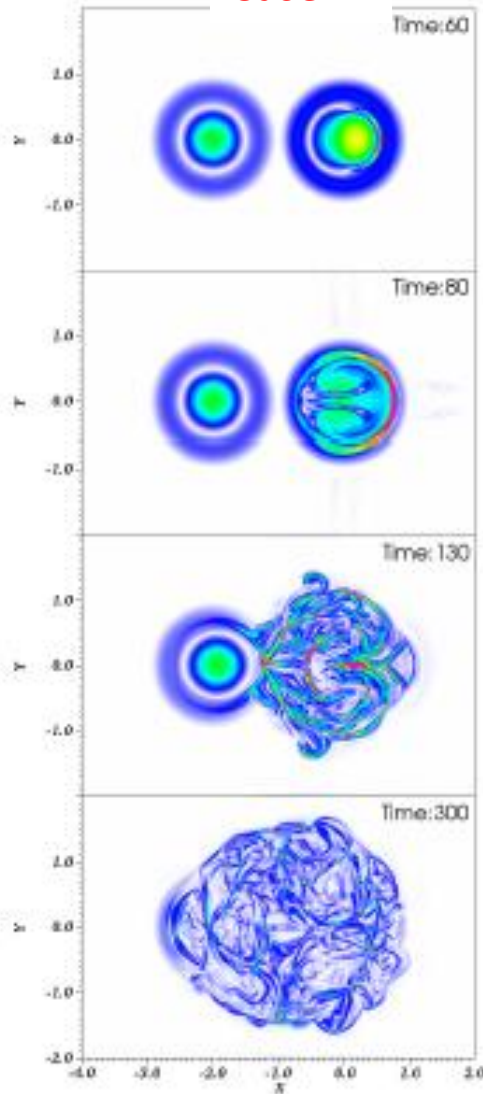
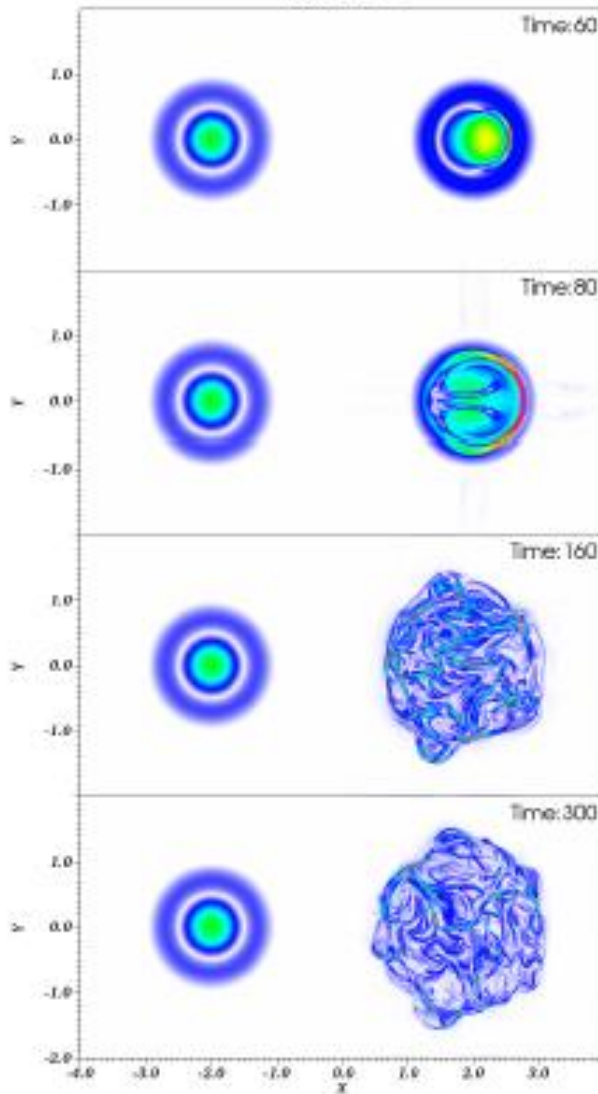
Unstable
loop

Case 3

Stable
loop

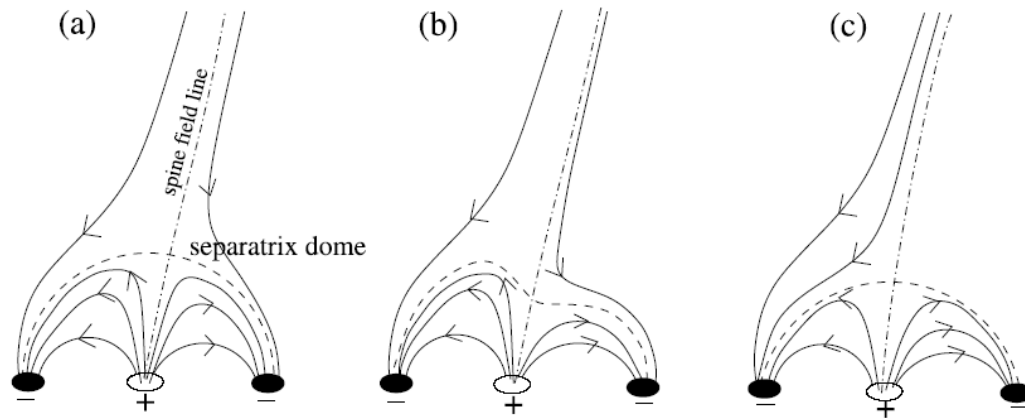
Unstable
loop

Case 4



Magnetic energy
versus time

3D null points in reconstructions of coronal field in flares



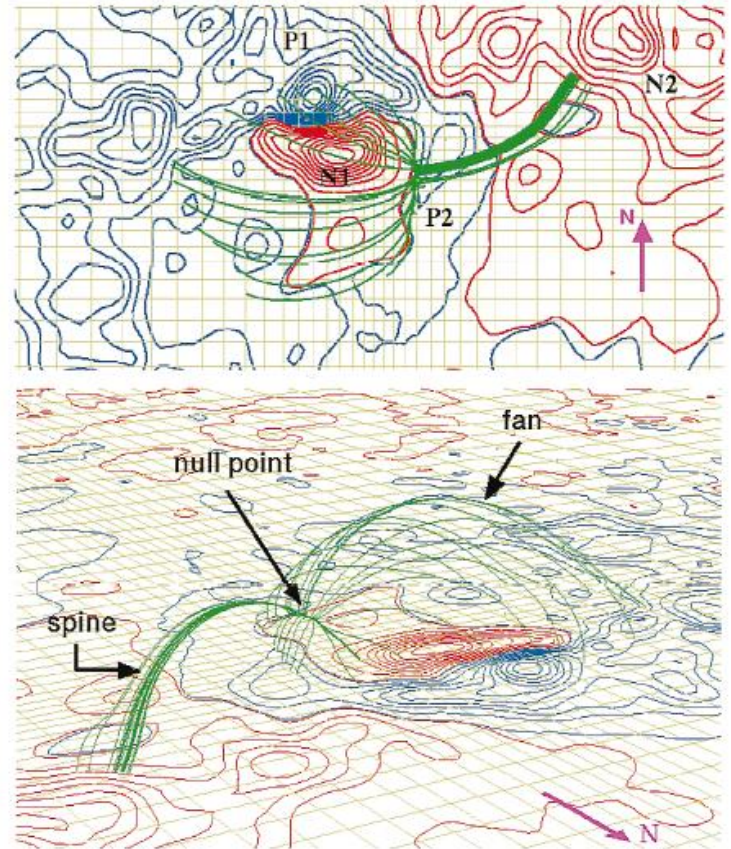
Fletcher et al 2001

Also:

Filippov, 1999, DesJardins et al 2009, Sun et al 2012, Sun et al 2014...

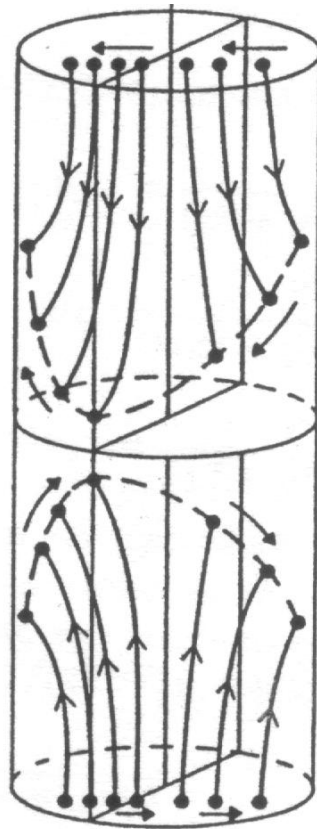
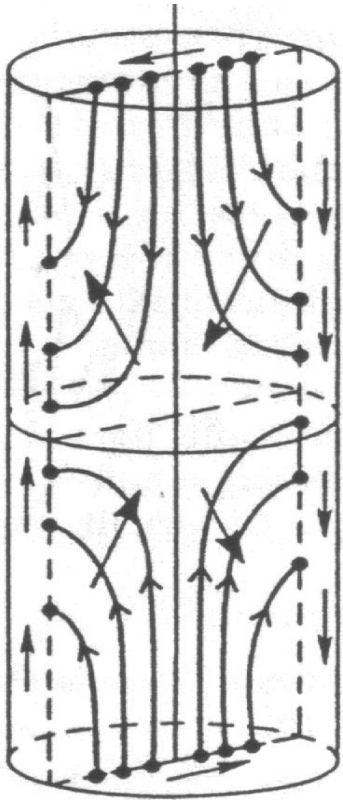
Data-driven simulation of flare ribbons with coronal null point *Masson et al 2009*

Also in magnetosphere e.g. *Xiao et al 2006...*



Aulanier et al 2000

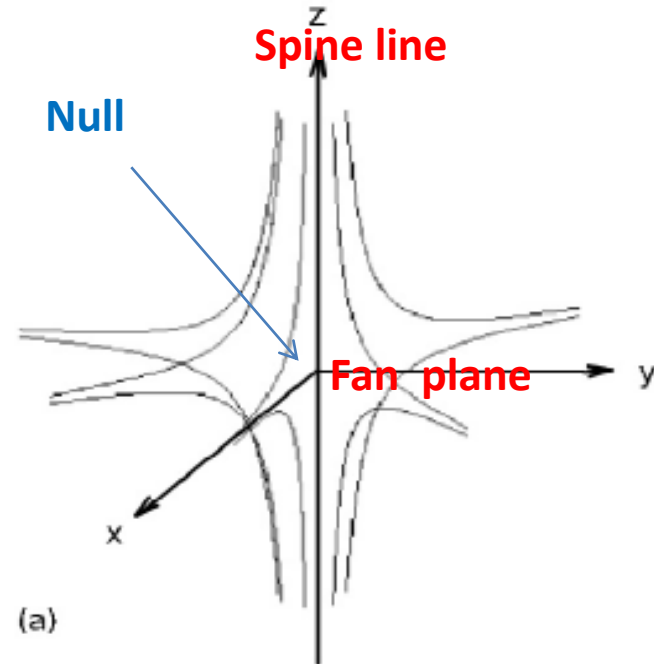
3D null points and reconnection



Spine reconnection

Fan reconnection

From Priest and Titov 1996



- Priest and Titov (1996) - **kinematic** solutions of **outer ideal reconnection region**
- Singularities (current tubes/sheets) at spine line or fan plane

Particle acceleration at reconnecting 3D nulls

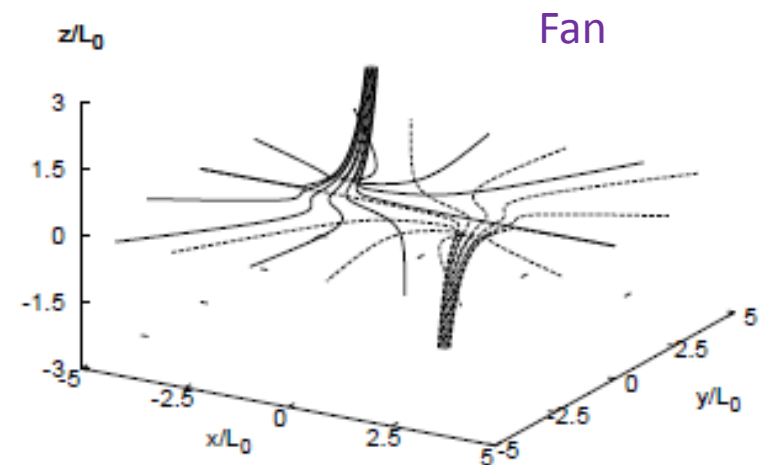
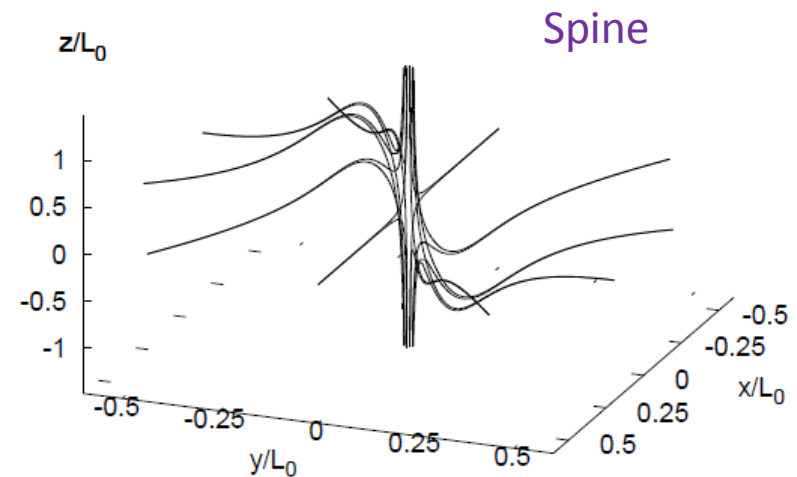
- Fields from simple models of outer ideal reconnection region – *Dalla and Browning, 2005, 2006, 2008; Browning et al 2010*
- Numerical simulation of 3D null – convective electric field only – *Guo et al (2010)*
- Stanier et al use background fields from exact solutions of steady MHD equations (Craig and Fabling, 1996, Craig et al 1997....)

$$\mathbf{B} = \lambda \mathbf{P} + Q(x, y) \hat{\mathbf{z}},$$

$$\mathbf{v} = \mathbf{P} + \lambda Q(x, y) \hat{\mathbf{z}},$$

Potential null + reconnection field

Q expressed in terms of Kummer functions

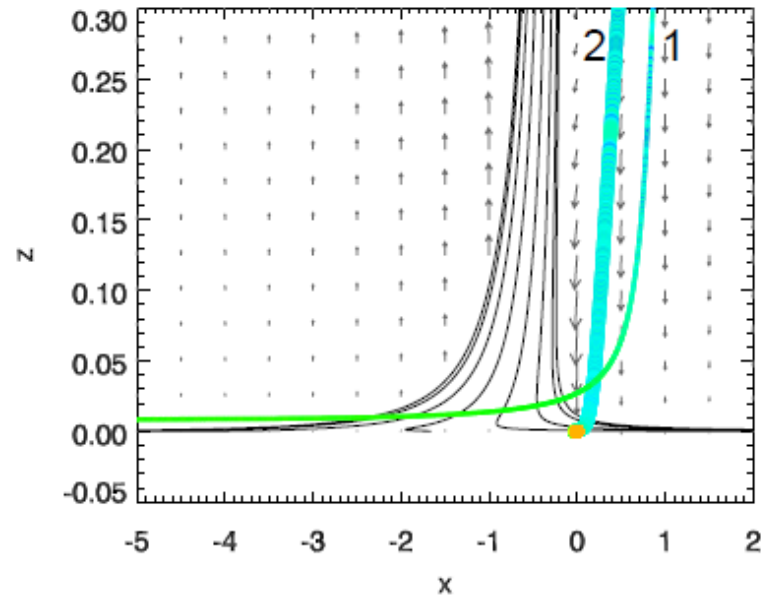
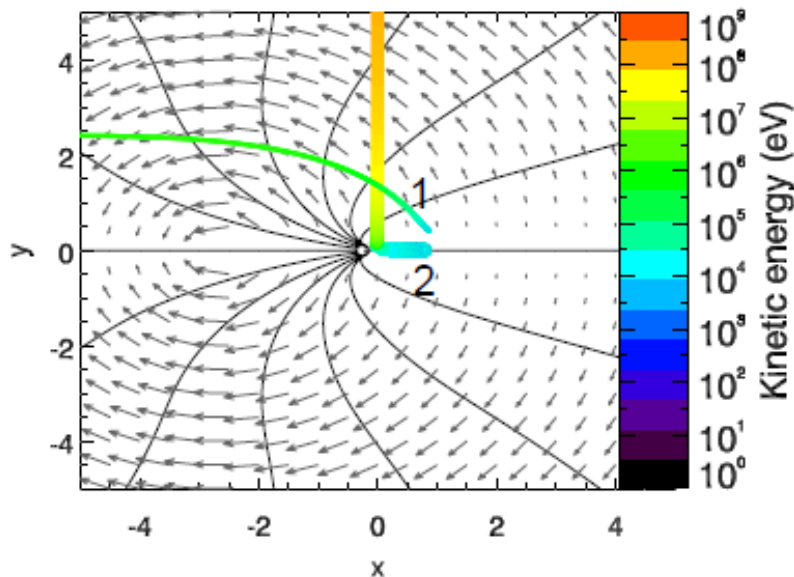


Proton trajectories in fan reconnection

– self-consistent C&F fields

- Electric field from $\mathbf{E} = -\mathbf{v} \times \mathbf{B} - \eta \mathbf{j}$
- Calculate test particle trajectories for ions using full Lorentz equations

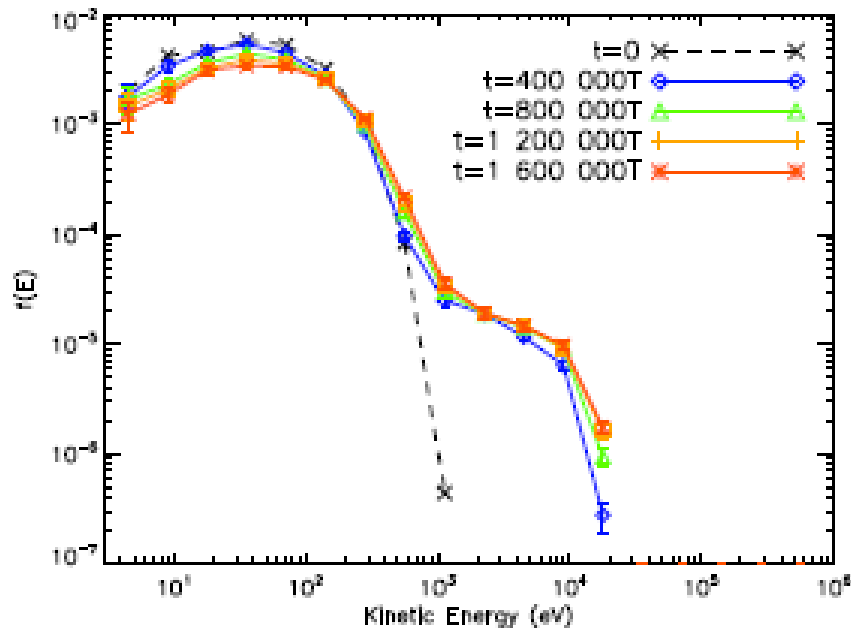
Stanier et al A&A 2012



- Typical energetic proton “1” – remains magnetised – gets close to current sheet but does not enter it
- Proton “2” enters current sheet and is directly accelerated – not ejected
- C.f. approximate solution near null *Litvinenko 2006*

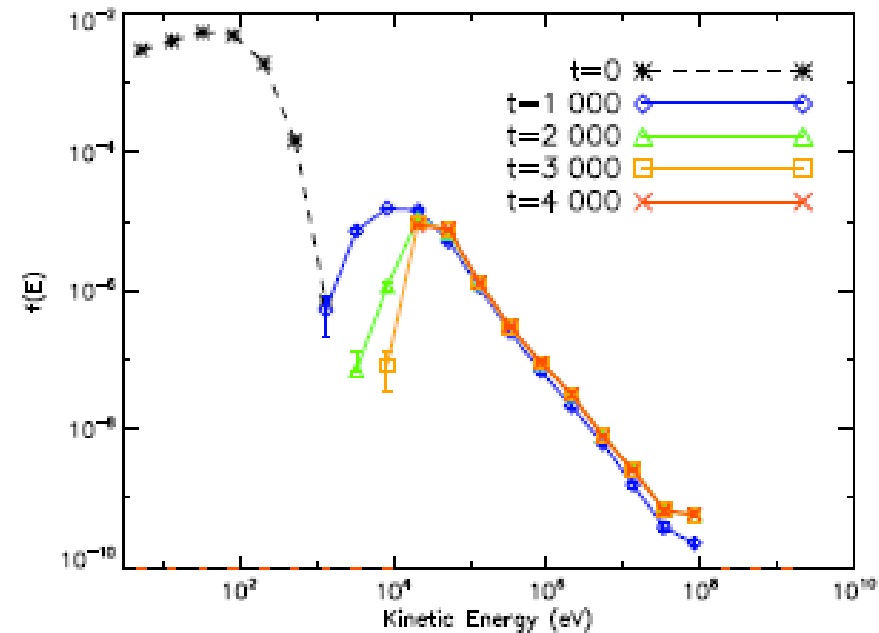
Proton energy spectra

Stanier et al A&A 2012



Spine case –

Some acceleration but rather weak
due to “flux pile up” limits on electric
field, small volume of spine
reconnection region



Fan case –

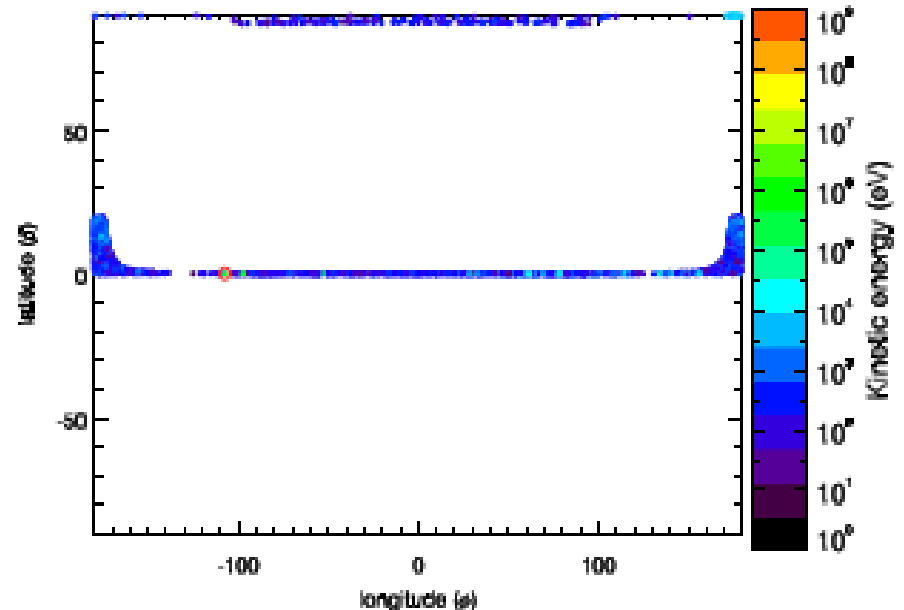
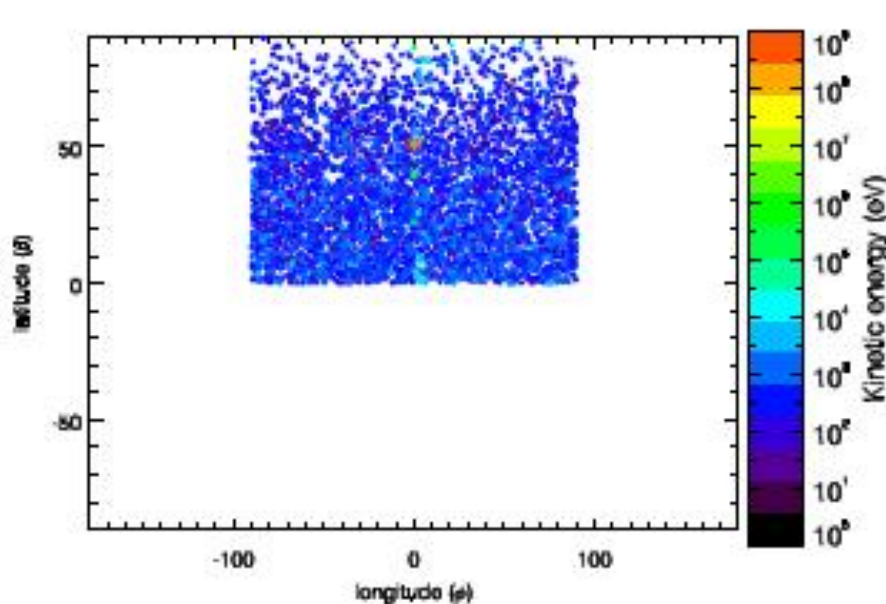
Almost all particles accelerated,
mainly due to strong electric drift
Unbounded current sheet

Electron acceleration

- Developed new “switching” particle solver:
 - Full Lorentz equations when Larmor radius too large
 - Guiding-centre when Larmor radius small
- 5000 electrons in C&F fan reconnection field, initially Maxwellian 86 eV, random pitch angles and gyrophase, uniformly distributed at global distance L from null
- Two populations – those with initially $y < 0$ are trapped close to spine and do not reach current sheet region – those with $y > 0$ are accelerated at low latitudes and escape
- Trapped population behaviour is caused by “reverse” parallel electric fields outside current sheet - effect on electrons is much stronger than for protons ($\sim 1/m$)
- Undertake simulations with much lower - and more realistic – values of η to reduce effect of reverse electric field

Energies and positions of electrons – reduced resistivity

$$\eta = 10^{-10} \quad \alpha = B_s = 5$$

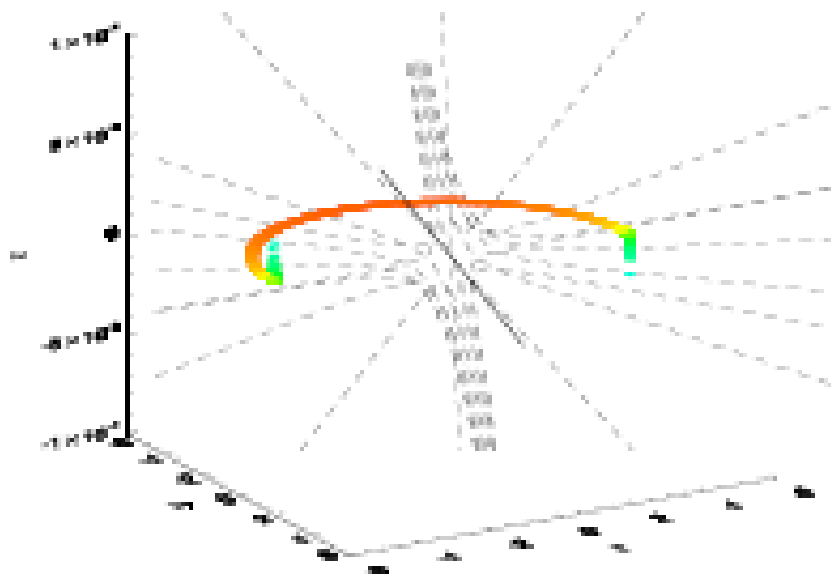


Initial positions
Colour coded by final energy

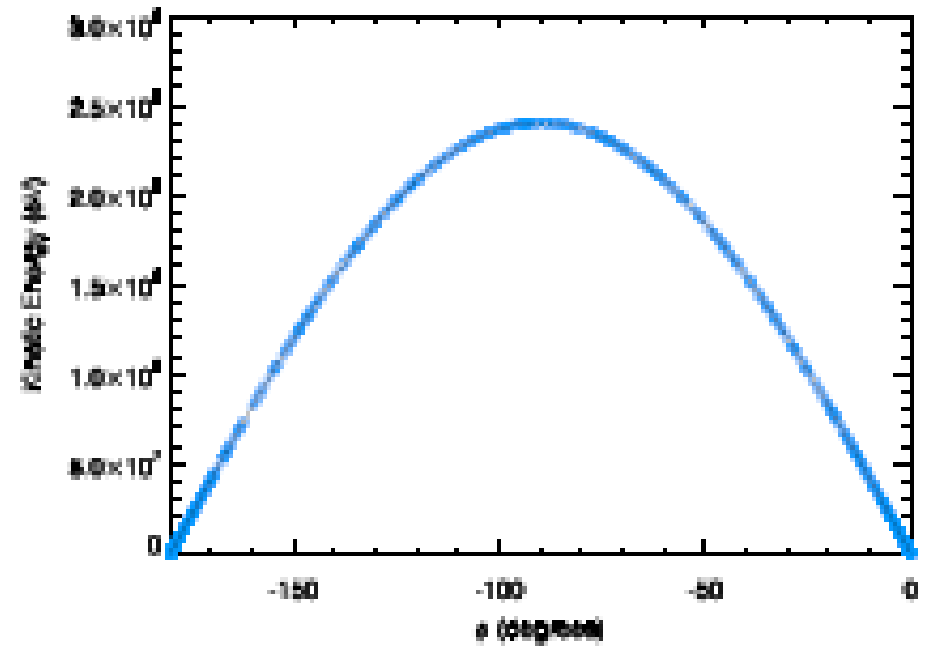
Final positions
Colour coded by final energy

Highest energy electron (red circled)
gets to 0.23 MeV

Electrons started in current sheet



a)



b)

$$t = 10^7 T_{c,e}$$

Stanier PhD thesis 2013

Observational predictions

- spatial locations of high-energy protons (> 1 MeV, orange)
and electrons (> 10 keV, blue)

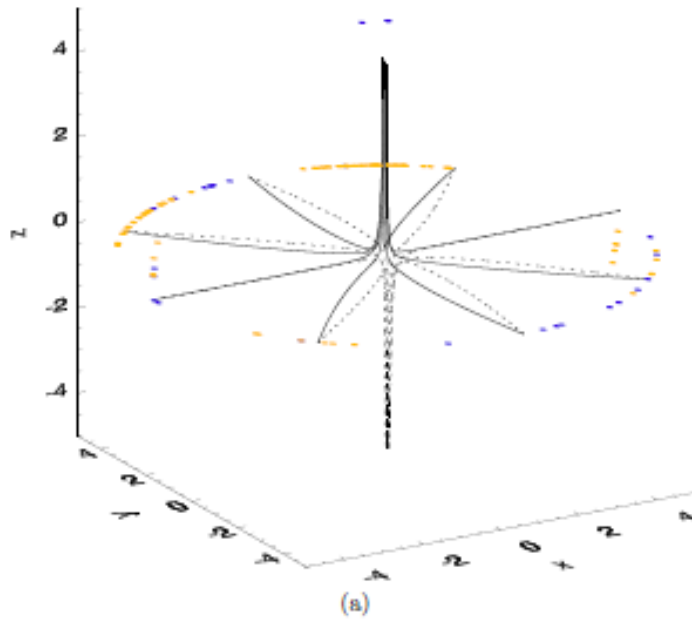
$$\eta = 10^{-10} \quad \alpha = B_s = 5$$

$$\lambda = 0.5$$

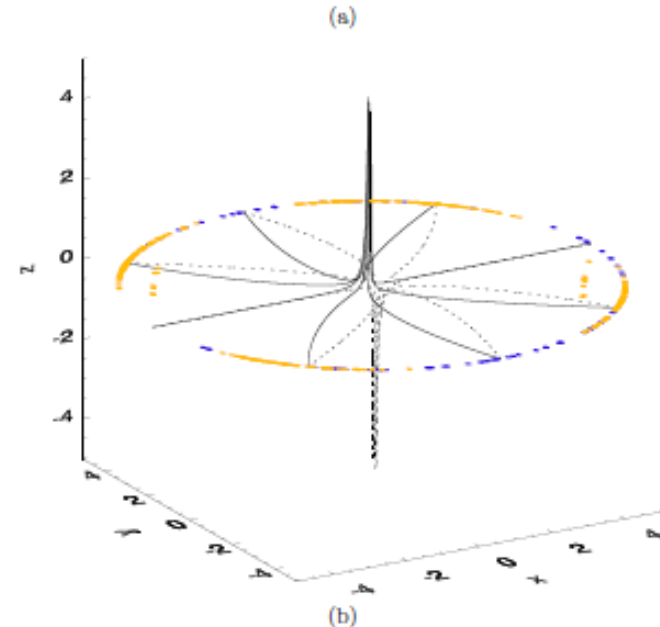
$$t = 0.4 \text{ s}$$

$$\lambda = 0.25$$

$$t = 0.2 \text{ s}$$



Protons
Electrons



Varying shear parameter λ

Energy spectra

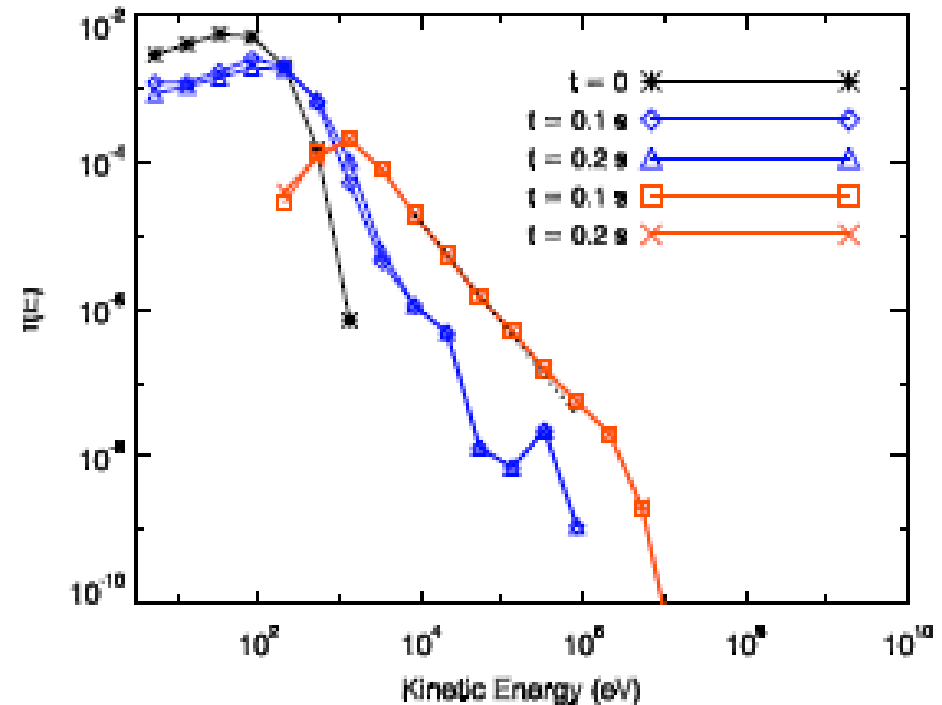
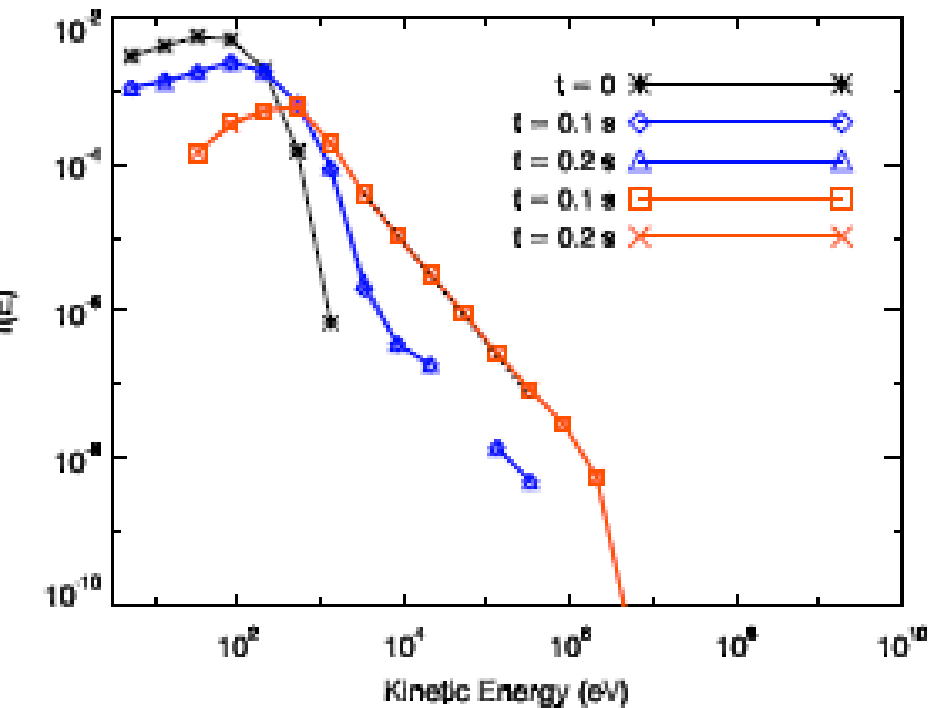
– protons (red) and electrons (blue)

$$\eta = 10^{-10}$$

$$\alpha = B_s = 5$$

$$\lambda = 0.5$$

$$\lambda = 0.25$$



Protons
Electrons

Summary

- The solar corona may be heated to millions of degrees by dissipation of stored magnetic energy through multiple magnetic reconnections
- Relaxation and release of stored magnetic energy may be triggered by ideal kink instability in twisted coronal loops
- 3D numerical simulations show formation of fragmented current sheet with multiple reconnections in nonlinear phase of kink instability
- Fast reconnection in the fragmented current sheet results in plasma heating and particle acceleration distributed throughout the loop volume
- We have simulated this in realistic curved coronal loops twisted by footpoint motions – representing a confined flare - and calculated observable signatures
- Repeated driving and relaxation gives a distribution of heating events of different magnitudes – may be power laws
- Instability in one loop may trigger relaxation in an unstable neighbour leading to an “avalanche” of heating events - heating may also result from merging of twisted filaments
- As a first step to more complex topologies, we have investigated particle acceleration at 3D magnetic null points